Acta Cryst E CRYSTALLOGRAPHIC COMMUNICATIONS

ISSN 2056-9890

Crystal structures and conformational features of new forms of tinidazole

Valeryia Hushcha,[a,b] Justyna Dominikowska[b] and Lilianna Chęcińska[b]*

[a]University of Lodz Doctoral School of Exact and Natural Sciences, Narutowicza 68, 90-136 Łódź, Poland, and [b]University of Lodz, Faculty of Chemistry, Pomorska 163/165, 90-236 Łódź, Poland. *Correspondence e-mail: lilianna.checinska@chemia.uni.lodz.pl

Received 5 November 2025
Accepted 12 November 2025

Edited by L. Van Meervelt, Katholieke Universiteit Leuven, Belgium

Keywords: tinidazole; crystal structure; polymorph; interaction energy; conformers.

CCDC references: 2502468; 2502467; 2502466

Supporting information: this article has supporting information at journals.iucr.org/e

The crystal structures of two new tinidazole {1-[2-(ethanesulfonyl)ethyl]-2-methyl-5-nitro-1*H*-imidazole, TNZ, $C_8H_{13}N_3O_4S$} forms, triclinic and hemihydrate, have been determined and compared to that of the known monoclinic form. The triclinic and hemihydrate structures each contain two independent molecules with similar conformations, whereas the monoclinic form adopts a distinct geometry. The conformational differences arise mainly from variations in the N—C—C—S torsion angle. A conformational study confirmed two preferred types of molecular conformations characteristic of tinidazole polymorphs. Interaction-energy analysis indicates that, despite differences in the crystal packing of the monoclinic and triclinic polymorphs, dispersion forces play a major role in consolidation of their structures.

1. Chemical context

The introduction of nitroheterocyclic drugs in the late 1950s and the 1960s marked a new era in the treatment of infections caused by both Gram-negative and Gram-positive bacteria, as well as a range of pathogenic protozoan parasites. Azomycin, a 2-nitroimidazole antibiotic isolated from a *Streptomyces* bacteria, was the first active nitroimidazole to be discovered (Nakamura *et al.*, 1955). It served as the primary impetus for the systematic search for drugs with activity against anaerobic protozoa. Research into alternative 5-nitroimidazoles began shortly after the introduction of metronidazole, aiming to develop compounds with similar efficacy but improved properties, such as enhanced compliance, longer serum half-life, and better safety profiles.

Tinidazole, 1-(2-ethylsulfonylethyl)-2-methyl-5-nitro-imidazole (TNZ), synthesized in 1969, has been widely used across Europe and developing countries for the treatment of parasites, mycobacteria, and Gram-positive and Gram-negative bacteria (Ang *et al.*, 2017). It was approved by the United States Food and Drug Administration (U.S. FDA) in 2004 for the treatment of trichomoniasis, giardiasis, amebiasis, and amoebic liver abscess (Sawyer *et al.*, 1976; Fung & Doan, 2005). Tinidazole has emerged as the most successful among these alternative 5-nitroimidazoles and demonstrates superiority over metronidazole in several respects. It shares a similar antimicrobial spectrum, has a longer half-life, and is better tolerated by patients (Wood & Monro, 1975; Crowell *et al.*, 2003; Fung & Doan, 2005). Most importantly, tinidazole can be effective in overcoming metronidazole resistance in many cases (Gardner & Hill, 2001).

In this study, the crystal structures of three forms of tinidazole: monoclinic, triclinic and hemihydrate, are described and compared, with emphasis on the molecular conformations

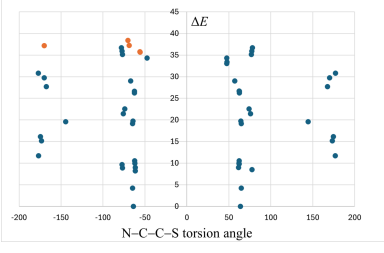

and the intermolecular interactions that govern the packing and stability of each polymorph.

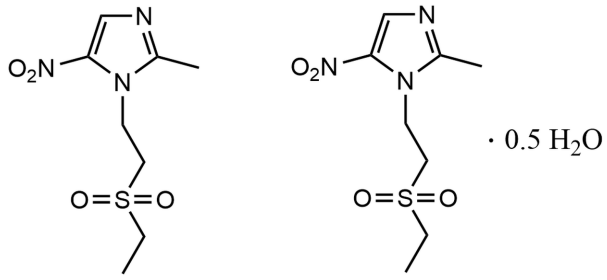

2. Structural commentary, conformational analysis and database survey

Fig. 1*a*–*c* presents the molecular structures of the three pure forms of tinidazole: the monoclinic, triclinic, and hemihydrate forms. In the triclinic and hemihydrate structures, two independent molecules are present, which exhibit highly similar molecular conformations (Fig. 2*a*). An overlay of all five independent tinidazole molecules shows that the monoclinic form significantly differs from the others.

A search of the Cambridge Structural Database (CSD version 6.00, April 2025; Groom *et al.*, 2016) revealed eight other additional tinidazole molecules adopting conformations similar to the two observed here (Fig. 2*b*). Structural analysis of the imidazole valence angle (C—N—C) indicated that only two of these molecules are protonated, with an angle of approximately 109°, whereas the remaining forms are neutral,

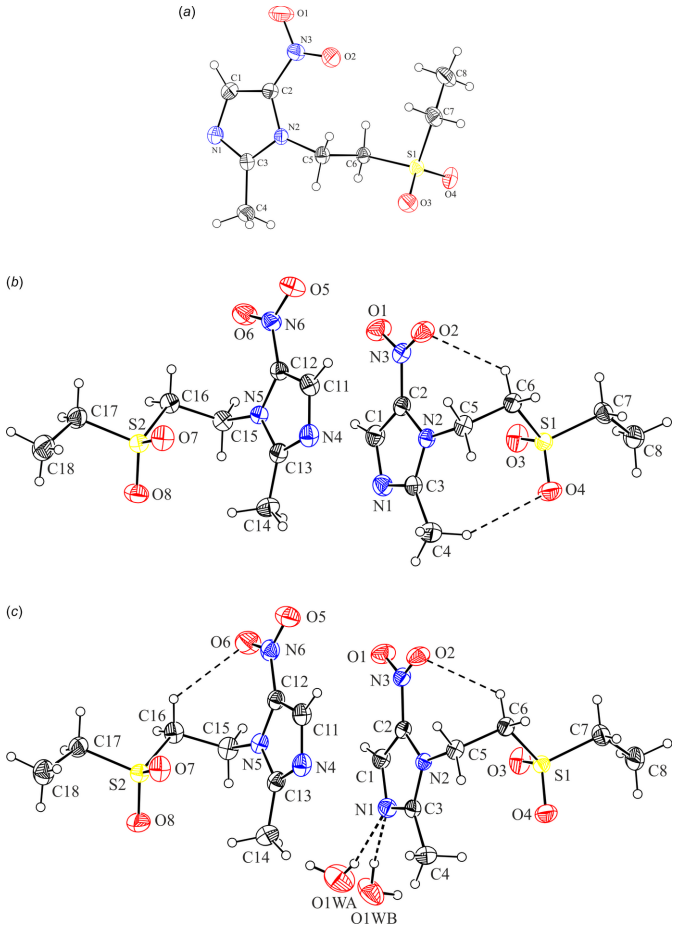

Figure 1
Views of the asymmetric unit of (*a*) TNZ-monoclinic, (*b*) TNZ-triclinic and (*c*) TNZ-hemihydrate, with the atom-numbering schemes. Displacement ellipsoids are drawn at the 30% probability level. H atoms are shown as spheres of arbitrary radii. The disorder components (*A* and *B*) of the water molecule have equal site occupancies (1/2).

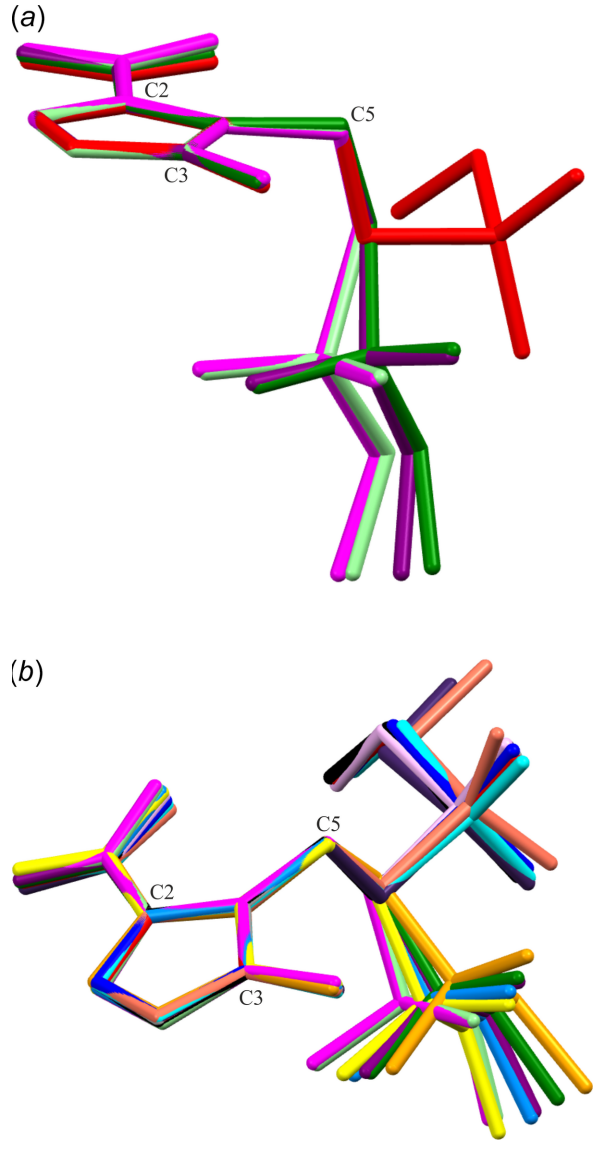

Figure 2
An overlay of (*a*) five tinidazole molecules, with colour codes: red – TNZ-monoclinic, light green – TNZ-triclinic (molecule 1), green – TNZ-triclinic (molecule 2), magenta – TNZ-hemihydrate (molecule 1), purple – TNZ-hemihydrate (molecule 2); and (*b*) additional ten tinidazole molecules from the CSD, with colour codes: CEPSIZ (Chasseaud *et al.*, 1984) – dark grey, CIPSIZ01 (Zheng *et al.*, 2020) – black, FISLE (Alfaro-Fuentesa *et al.*, 2014) – orange, MUKXIC (Fandino *et al.*, 2020) – cyan, MUKXOI (Fandino *et al.*, 2020) – blue, NIJCES (Li *et al.*, 2023) – yellow, NIJCIW (Li *et al.*, 2023) – pink, NIJCOC (Li *et al.*, 2023) – navy blue, PUZDEW (molecule 1) (Zheng *et al.*, 2020) – dark purple, PUZDEW (molecule 2) (Zheng *et al.*, 2020) – salmon. Atoms C2, C3 and C5 have been used for the overlay.

Table 1
Selected geometric parameters (Å, °) for TNZ molecules.

TNZ(1) and TNZ(2) – independent TNZ molecules from the asymmetric unit.

Structure/Refcode	Study temp. (K)	C3—N1—C1/ C13—N4—C11	C2—N2—C5—C6/ C12—N5—C15—C16	C3—N2—C5—C6/ C13—N5—C15—C16	N2—C5—C6—S1/ N5—C15—C16—S2
TNZ-triclinic(1)	294	105.66 (17)	–64.0 (2)	109.6 (2)	–56.1 (2)
TNZ-triclinic(2)	294	106.46 (17)	–69.7 (2)	107.0 (2)	–70.36 (19)
TNZ-hemihydrate(1)	294	106.6 (3)	–63.1 (4)	109.5 (4)	–55.9 (4)
TNZ-hemihydrate(2)	294	106.8 (3)	–69.6 (5)	106.1 (4)	–68.8 (4)
TNZ-monoclinic	294	105.83 (12)	–77.93 (16)	97.29 (15)	170.06 (8)
CEPSIZ (TNZ-monoclinic)	295	105.6	–77.5	97.3	170.1
CEPSIZ01 (TNZ-monoclinic)	100	105.9	75.9	–98.3	–169.5
FISLIE	293	109.9	75.3	–108.4	75.7
MUKXIC	173	106.6	81.5	–97.6	–173.0
MUKXOI	173	107.0	67.6	–105.9	66.9
NIJCES	293	109.8	–69.5	104.0	–61.7
NIJCIW	293	106.6	78.9	–98.9	–167.0
NIJCOC	293	107.0	–80.6	99.9	169.8
PUZDEW	100	106.6	–82.4	100.7	173.9
PUZDEW	100	106.2	81.5	–94.6	–165.6

with the C—N—C angle ranging from 105.6° for TNZ-monoclinic (CEPSIZ; Chasseaud *et al.*, 1984) to 107.0° for NIJCOC (Li *et al.* 2023) (Table 1). The two conformational types can be distinguished by the torsion angle N2—C5—C6—S1/N5—C15—C16—S2, which is approximately ±55–70° in the triclinic and the hemihydrate forms, and ±170° in the monoclinic polymorph. One may say that in the triclinic and the hemihydrate forms, TNZ adopts a conformation close to *gauche* rotamers, whilst the monoclinic polymorph contains TNZ rotamers being close to the anti-periplanar conformation.

In this study, we performed a detailed conformational analysis of the tinidazole molecule based on the experimental crystal structures of its monoclinic and triclinic forms. For this purpose, we determined the crystal structure of the monoclinic form, although it had previously been reported by Chasseaud *et al.* (1984) and by Zheng *et al.* (2020).

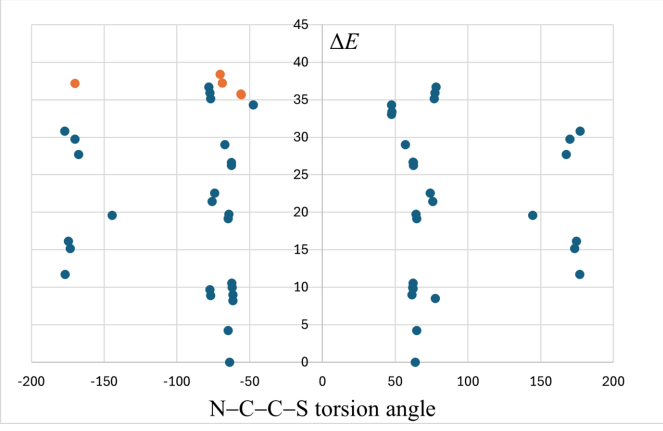

Figure 3
Relative energy values (ΔE in kJ mol^{-1}) plotted against the N—C—C—S angle (°). Conformers of TNZ generated in the conformational analysis are shown in navy blue; conformers present in the crystal structures of TNZ-monoclinic, TNZ-triclinic and TNZ-hemihydrate in orange.

The geometry optimization at the DFT theory level performed for the generated possible conformers yielded 54 conformers, approximately half of which were found to be unique after evaluation of their relative energies and the sign of the key torsion angle of N—C—C—S. In Fig. 3 one may notice that, similar to the results of the CSD survey, the obtained conformers can be classified into two groups, namely the one in which the torsion angle N—C—C—S adopts values about ±60° (40 conformers), being close to *gauche* rotamers, and the group in which the values of the N—C—C—S angle are about ±170° (14 conformers), being close to the anti-periplanar rotamer. The energy values for the studied conformers are given in Table S1 in the supporting information. The relative energy values, ΔE, for studied conformers range up to 36.7 kJ mol^{-1} and they do not differ significantly for the two main groups of rotamers described above. One may also analyse relative energy values for TNZ in its three forms found in the crystal structure, namely in the monoclinic, triclinic and hemihydrate forms (Table S2 in the supporting information). In this case relative energies are smaller than 2.8 kJ mol^{-1}, indicating that the conformers of TNZ present in the crystal structure hardly differ in energy.

3. Supramolecular features

In this study, we compare the supramolecular architectures of two polymorphs of tinidazole: TNZ-monoclinic and TNZ-triclinic, at room temperature. The analysis is based on interaction energies calculated using the pairwise model implemented in *CrystalExplorer* (Spackman *et al.*, 2021). Pairwise model energies (Turner *et al.*, 2014) were estimated and visualized (Turner *et al.*, 2015; Mackenzie *et al.*, 2017) for molecular pairs within a cluster of a radius of 3.8 Å, using a B3LYP/6-31G(d,p) molecular wave function. The total interaction energy between nearest-neighbour molecular pairs was decomposed into four components: electrostatic, polarization, dispersion and exchange-repulsion with scale factors of 1.057, 0.740, 0,871 and 0.618, respectively.

Table 2
Interaction energies (kJ mol^{-1}) for selected molecular pairs.

TNZ(1) and TNZ(2) – independent TNZ molecules from the asymmetric unit. N is the number of molecular pairs. R is the distance (Å) between molecular centroids. E_{tot} is the total energy and its individual components: E_{ele} is electrostatic (k = 1.057), E_{pol} is polarization (k = 0.740), E_{dis} is dispersion (k = 0.871), E_{rep} is repulsion (k = 0.618).

Structure	Molecular pair	Interaction	kE_{ele}	kE_{pol}	kE_{dis}	kE_{rep}	kE_{tot}
TNZ-monoclinic	TNZ–TNZ	C1—H1···O1^{i}	–12.8	–1.3	–6.8	9.0	–11.9
	TNZ–TNZ	C6—H6*A*···O3^{ii}	–11.2	–4.0	–27.5	12.0	–30.6
	TNZ–TNZ	C6—H6*B*···O3^{iii}	–47.2	–8.7	–37.4	18.8	–64.6
TNZ-triclinic	TNZ(1)–TNZ(1)	C1—H1···N4^{i}	–20.4	–3.3	–9.5	15.5	–17.7
	TNZ(2)–TNZ(2)	C16—H16*A*···O7^{i}	–17.3	–4.0	–21.8	14.6	–28.5
	TNZ(1)–TNZ(2)	*Cg*(1)···*Cg*(2)	–7.5	–1.9	–32.1	11.0	–30.5

Symmetry codes: TNZ-monoclinic (i) $-x+1, -y+2, -z+1$; (ii) $x, y+1, z$; (iii) $-x, -y, -z+1$. TNZ-triclinic: (i) $x+1, y, z$.

Table 3
Hydrogen-bond geometry (Å, °) for TNZ-monoclinic.

D—H···*A*	*D*—H	H···*A*	*D*···*A*	*D*—H···*A*
C1—H1···O1^{i}	0.93	2.45	3.374 (2)	171
C6—H6*A*···O3^{ii}	0.97	2.53	3.3777 (17)	146
C6—H6*B*···O3^{iii}	0.97	2.53	3.2942 (17)	136

Symmetry codes: (i) $-x+1, -y+2, -z+1$; (ii) $x, y+1, z$; (iii) $-x, -y, -z+1$.

Table 4
Hydrogen-bond geometry (Å, °) for TNZ-triclinic.

D—H···*A*	*D*—H	H···*A*	*D*···*A*	*D*—H···*A*
C1—H1···N4^{i}	0.93	2.39	3.319 (3)	174
C4—H4*C*···O4	0.96	2.51	3.365 (3)	148
C6—H6*B*···O2	0.97	2.41	3.057 (3)	124
C16—H16*A*···O7^{i}	0.97	2.34	3.177 (2)	145

Symmetry code: (i) $x+1, y, z$.

The crystal structure of the monoclinic form of tinidazole was previously reported by Zheng *et al.* (2020), including interaction energy analysis at 100 K. The agreement between the interaction energies obtained for the room- and low-temperature models is very good, differing by only a few kJ mol^{-1}, which can be attributed solely to geometric variations. Nevertheless, this analysis was repeated here to enable direct comparison with the triclinic form, which was found to be unstable at low temperature. The hydrogen-bonding scheme proposed by Zheng *et al.* is very detailed; however in the present work, only the shortest hydrogen bonds with proton···acceptor distances shorter by 0.15 Å than the sum of van der Waals radii of the interacting atoms were considered. This approach ensures a consistent interpretation of the supramolecular architectures of both polymorphs.

Table 2 lists selected interaction energies for molecular pairs connected by hydrogen bonds, as summarized in Tables 3 and 4 for TNZ-monoclinic and TNZ-triclinic, respectively. Complete interaction energy data are provided in Tables S4 and S5 in the supporting information. The pairwise model analysis was not performed for the TNZ-hemihydrate structure because the positional disorder of the water molecule complicated such calculations.

In the crystal structure of TNZ-monoclinic, three C—H···O hydrogen bonds are observed (Table 3). In two of these interactions, atom C6 acts as the donor and atom O3 as an acceptor. The C6—H6*A*···O3($x, y+1, z$) interaction forms a *C*(4) chain motif running along the [010] direction, while the C6—H6*B*···O3($-x, -y, -z+1$) interaction generates an $R_2^2(8)$ motif (Etter, 1990; Etter *et al.*, 1990; Bernstein *et al.*, 1995). The combination of these two hydrogen bonds results in a finite pattern of $R_4^2(8)$ motifs, constructing a chain of edge-fused centrosymmetric rings (Fig. 4*a*). The total interaction energies of these two C—H···O contacts are −30.6 and −64.6 kJ mol^{-1}, respectively. The most linear interaction, C1—H1···O1($-x+1, -y+2, -z+1$), is responsible for the formation of centrosymmetric dimers with an $R_2^2(10)$ motif

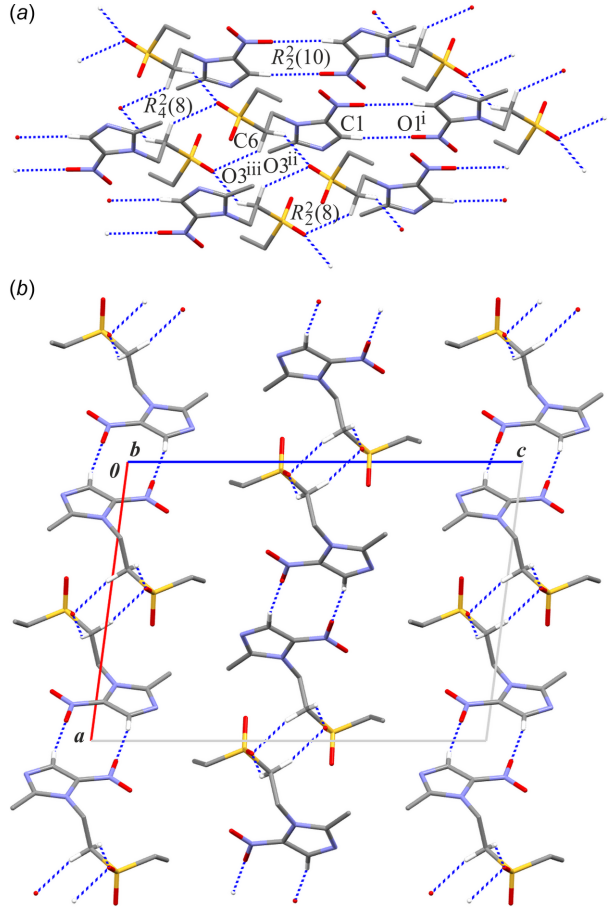

Figure 4
A part of the crystal structure of TNZ-monoclinic showing (*a*) a scheme of interactions and (*b*) an arrangement of di-periodic layers in a view along the *b* axis. Hydrogen bonds are drawn as dashed lines and (C)—H atoms not involved in hydrogen bonds have been omitted. Symmetry codes: (i) $-x+1, -y+2, -z+1$; (ii) $x, y+1, z$; (iii) $-x, -y, -z+1$.

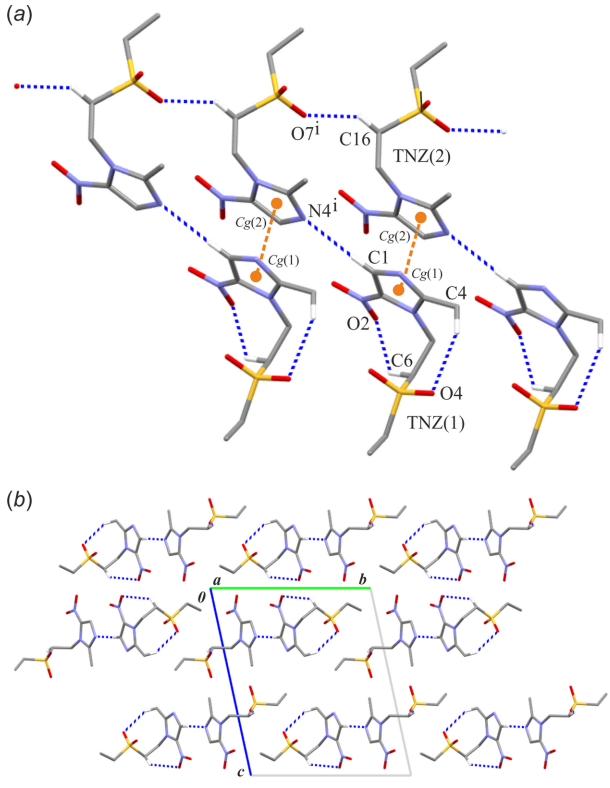

Figure 5
A part of the crystal structure of TNZ-triclinic showing (*a*) a scheme of interactions and (*b*) an arrangement of mono-periodic ribbons in a view along the *a* axis. Hydrogen bonds are drawn as blue dashed lines and (C)—H atoms not involved in hydrogen bonds have been omitted. Orange balls correspond to the centre of gravity of the imidazole rings [denoted *Cg*(1) and *Cg*(2)]. Orange dashed lines represent aromatic π–π interactions. Symmetry code: (i) $x + 1, y, z$.

(E_{tot}=–11.9 kJ mol^{-1}). This interaction links the aforementioned chain of rings along the [100] direction. As a result, supramolecular di-periodic layers are formed, lying parallel to the (001) plane (Fig. 4*b*). No other direction-specific interactions are observed between the layers.

In the crystal structure of TNZ-triclinic, two independent TNZ molecules are present in the asymmetric unit (Fig. 1*b*). The molecular structure of TNZ(1) molecule features two intramolecular hydrogen bonds: C4—H4*C*···O4 and C6—H6*B*···O2 (Table 4). In addition, there are two intermolecular hydrogen bonds of the C—H···O/N types. The C16—H16*A*···O7($x + 1, y, z$) interaction generates a *C*(4) chain motif built from TNZ(2) molecules and running along the [100] direction (E_{tot}=–28.5 kJ mol^{-1}). TNZ(1) molecules bind to this chain *via* the C1—H1···N4($x + 1, y, z$) interaction (E_{tot}=–17.7 kJ mol^{-1}), forming finite D-type motifs (Fig. 5*a*). As a result, supramolecular mono-periodic ribbons are formed. Within these ribbons, aromatic π–π stacking interactions occur between the imidazole rings of the independent tinidazole molecules (1) and (2) from the asymmetric unit (Table S3 in the supporting information). This aromatic interaction exhibits the total energy of −30.5 kJ mol^{-1}, dominated by the highest dispersion contribution of −32.1 kJ mol^{-1}. No direction-specific interactions are observed between the ribbon assemblies (Fig. 5*b*).

In summary, comparison of the two polymorphs of tinidazole from an energetic perspective shows that the highest total interaction energies occur in the monoclinic form (up to approximately −60 kJ mol^{-1}), compared with less than −40 kJ mol^{-1} in the triclinic form, although both structures feature only C—H···O/N hydrogen bonds. Interestingly, in both polymorphs, the ratio of electrostatic to dispersion energy

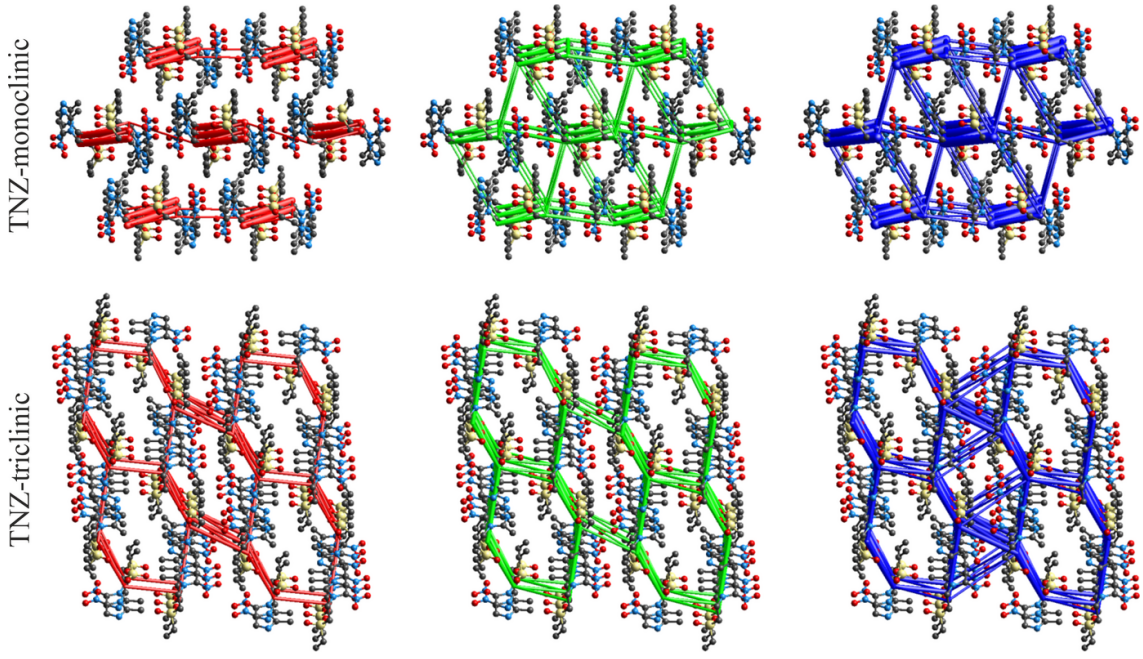

Figure 6
The representative energy framework diagrams for separate electrostatic (red) and dispersion (green) components, and the total interaction energy (blue) for TNZ-monoclinic (viewed along the *b* axis) and TNZ-triclinic (viewed along the *a* axis). All cylindrical radii are proportional to the relative strength of the corresponding energies and they were adjusted to the same scale factor of 80 with a cut-off value of −10 kJ mol^{-1}.

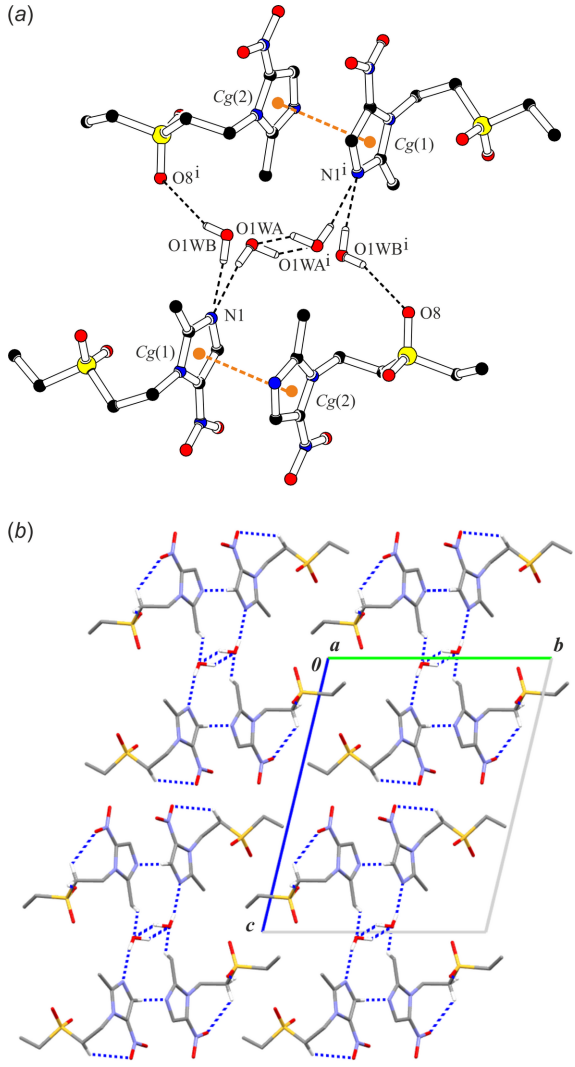

Figure 7
A part of the crystal structure of TNZ-hemihydrate showing (*a*) a scheme of hydrogen bonds to disordered *A* and *B* components of the water molecule and (*b*) a scheme of mono-periodic column-like assemblies in a view along the a axis (for clarity, disorder component *B* of the water molecule has been omitted). Hydrogen bonds are drawn as black dashed lines and (C)—H atoms not involved in hydrogen bonds have been omitted. Orange balls correspond to the centre of gravity of the imidazole rings [denoted *Cg*(1) and *Cg*(2)]. Orange dashed lines represent aromatic π-π- interactions. Symmetry code: (i) $-x+1, -y+1, -z$.

contributions summed over molecular pairs within the 3.8 Å cluster is the same, at approximately 40:60 (2:3). To put this result into perspective, in two isavuconazole polymorphs, the electrostatic-to-dispersive contribution ratio differs: being 25:75 for the monoclinic and 42:58 for the orthorhombic form, respectively (Ben & Chęcińska, 2025). The ratio 2:3 indicates that both supramolecular architectures are strongly influenced by non-directional dispersive interactions. This trend is reflected in the energetic frameworks, where the tri-periodic pattern of the total interaction energies corresponds with that found for the dispersion component (Fig. 6). The variety in the electrostatic component distribution is smaller for TNZ-triclinic, with its tri-periodic motif resembling that of the dispersion distribution, than in TNZ-monoclinic, in which the

Table 5
Hydrogen-bond geometry (Å, °) for TNZ-hemihydrate.

D—H···*A*	*D*—H	H···*A*	*D*···*A*	*D*—H···*A*
O1*WA*—H1*WB*···N1	0.85	2.09	2.908 (5)	162
O1*WB*—H1*WC*···N1	0.85	2.06	2.882 (5)	163
O1*WA*—H1*WA*···O1WA^{i}	0.85	1.44	2.180 (10)	143
O1*WB*—H1*WD*···O8^{i}	0.85	2.56	3.370 (5)	158
C1—H1···N4^{ii}	0.93	2.38	3.310 (3)	175
C6—H6*B*···O2	0.97	2.42	3.063 (2)	124
C14—H14*B*···O1*WA*^{i}	0.96	2.49	3.348 (6)	149
C15—H15*A*···O1*WB*^{i}	0.97	2.46	3.41 (4)	168
C16—H16*B*···O6	0.97	2.50	3.100 (3)	120
C16—H16*A*···O7^{ii}	0.97	2.37	3.183 (2)	141

Symmetry codes: (i) $-x+1, -y+1, -z$; (ii) $x+1, y, z$.

electrostatic distribution is essentially mono-periodic, being dominated by a single strong directional interaction.

In the crystal structure of TNZ-hemihydrate, each independent TNZ molecule features one short intramolecular hydrogen bond: C6—H6*B*···O2 in TNZ(1) and C16—H16*B*···O6 in TNZ(2), respectively (Fig. 1*c*; Table 5). As in TNZ-triclinic, supramolecular ribbons are formed through the C16—H16*A*···O7($x+1, y, z$) and C1—H1···N4($x+1, y, z$) interactions. Both components of the disordered water molecule participate in hydrogen bonding with tinidazole molecules *via* O1*WA*—H1*WB*···N1 (component *A*), and O1*WB*—H1*WC*···N1 and O1*WB*—H1*WD*···O8($-x+1, -y+1, -z$) (component *B*) interactions. Two additional C—H···O interactions: C14—H14*B*···O1*WA*($-x+1, -y+1, -z$) and C15—H15*A*···O1*WB*($-x+1, -y+1, -z$) further stabilize the molecular substructure (Fig. 7*a*). Finally, the ribbons doubled across the inversion centre form column-like assemblies (Fig. 7*b*). The aromatic π–π-interaction, *Cg*(1)···*Cg*(2), is preserved within the ribbon structure (Table S3 in the supporting information).

4. Hirshfeld surface analysis

Hirshfeld surface analysis (Spackman & McKinnon, 2002; Spackman & Jayatilaka, 2009) was performed using *CrystalExplorer* (Spackman *et al.*, 2021) to visualize and quantify intermolecular interactions in all three (solvato)polymorphs of tinidazole. As shown in the breakdown diagram (Fig. 8), the major contributions to the Hirshfeld surface in the described

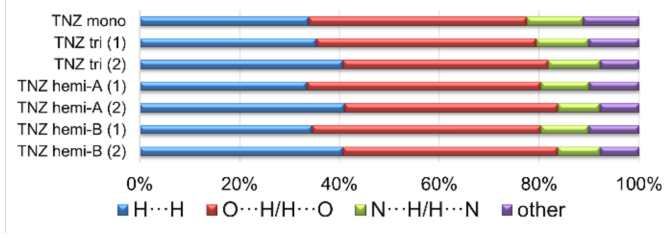

Figure 8
Diagram of percentage contributions of different close contacts to the Hirshfeld surface area of TNZ molecules in three analysed forms, including tinidazole molecules (1) and (2) and two positions of the disordered water molecule (*A* and *B*).

Table 6
Experimental details.

	TNZ-monoclinic	TNZ-triclinic	TNZ-hemihydrate
Crystal data			
Chemical formula	$C_8H_{13}N_3O_4S$	$C_8H_{13}N_3O_4S$	$C_8H_{13}N_3O_4S{\cdot}0.5H_2O$
M_r	247.27	247.27	256.28
Crystal system, space group	Monoclinic, $P2_1/n$	Triclinic, $P\overline{1}$	Triclinic, $P\overline{1}$
Temperature (K)	294	294	294
a, b, c (Å)	11.9943 (2), 5.5233 (1), 16.8454 (2)	5.7208 (2), 13.2759 (5), 15.5932 (5)	5.7223 (1), 13.1854 (2), 16.2439 (4)
α, β, γ (°)	90, 97.499 (1), 90	77.101 (3), 85.407 (2), 77.923 (3)	102.658 (2), 92.226 (2), 102.484 (2)
V (Å^3)	1106.43 (3)	1128.16 (7)	1162.76 (4)
Z	4	4	4
Radiation type	Cu $K\alpha$	Cu $K\alpha$	Cu $K\alpha$
μ (mm^{-1})	2.69	2.64	2.61
Crystal size (mm)	0.27 × 0.06 × 0.04	0.23 × 0.04 × 0.02	0.22 × 0.06 × 0.03
Data collection			
Diffractometer	Rigaku XtaLAB Synergy, Dual-flex, HyPix	Rigaku XtaLAB Synergy, Dual-flex, HyPix	Rigaku XtaLAB Synergy, Dual-flex, HyPix
Absorption correction	Gaussian (*CrysAlis PRO* 1.171.42.88a; Rigaku OD, 2023)	Gaussian (*CrysAlis PRO* 1.171.42.88a; Rigaku OD, 2023)	Gaussian (*CrysAlis PRO* 1.171.44.109a; Rigaku OD, 2025)
T_{min}, T_{max}	0.208, 1.000	0.496, 1.000	0.372, 1.000
No. of measured, independent and observed [$I > 2\sigma(I)$] reflections	10724, 2118, 2011	11280, 4260, 3758	11604, 4366, 3775
R_{int}	0.022	0.032	0.029
(sin $\theta/\lambda)_{max}$ (Å^{-1})	0.617	0.617	0.617
Refinement			
$R[F^2 > 2\sigma(F^2)]$, $wR(F^2)$, S	0.028, 0.081, 1.08	0.039, 0.103, 1.03	0.037, 0.101, 1.06
No. of reflections	2118	4260	4366
No. of parameters	148	293	311
H-atom treatment	H-atom parameters constrained	H-atom parameters constrained	H-atom parameters constrained
$\Delta\rho_{max}$, $\Delta\rho_{min}$ (e Å^{-3})	0.22, −0.22	0.20, −0.34	0.22, −0.34

Computer programs: *CrysAlis PRO* 1.171.42.88a and 1.171.44.109a (Rigaku OD, 2023, 2025), *SHELXT* (Sheldrick, 2015*a*), *SHELXL2019/2* and *SHELXL2019/3* (Sheldrick, 2015*b*), *Mercury* (Macrae *et al.*, 2020); *PLATON* (Spek, 2020) and *publCIF* (Westrip, 2010).

three forms arise from H···H and O···H/H···O contacts. These two types of interactions complement each other and together sum up approximately to 80% of the surface contributions (Figs. S1 and S2 in the supporting information). In the hemihydrate solvatomorph, the trend observed for the two independent molecules, TNZ(1) and TNZ(2), in the triclinic form is retained, with the proportion of O···H/H···O contacts increasing by only about 2%. In all three analysed structures, N···H/H···N contacts represent the third most significant contribution to the Hirshfeld surface of the TNZ molecules, amounting to roughly 10%. In the hemihydrate form, for TNZ(1), some of these contacts are shorter (represented by the longer spikes in Fig. S2 in the supporting information) than in the other forms, due to hydrogen bonding between TNZ(1) and both components of the disordered water molecule.

5. Synthesis and crystallization

The tinidazole (purity > 98%) used in this study was purchased from Angene Chemical (India), 4-nitrobenzoic acid (purity > 99%) was purchased from Sigma-Aldrich (USA).

All three forms of tinidazole were obtained during the attempted cocrystallization of the drug with 4-nitrobenzoic acid. For cocrystal synthesis, equimolar quantities (0.05 mmol of each) of tinidazole and 4-nitrobenzoic acid were ground together using a mortar and pestle. The resulting fine powder was then dissolved in ethanol and heated to 345 K. The solution was filtered and covered with perforated paraffin film. Finally, it was left to evaporate slowly at room temperature until crystals formed. Although cocrystals of tinidazole and 4-nitrobenzoic acid were not obtained, two new forms of tinidazole were identified: TNZ-hemihydrate and TNZ-triclinic, along with the known monoclinic form.

6. Refinement

Crystal data, data collection and structure refinement details are summarized in Table 6. All (C)—H atoms were placed geometrically and refined as a riding model with U_{iso}(H) = 1.2U_{eq}(C) for the methylene and aromatic groups, and 1.5U_{eq}(C) for the methyl group. During the refinement of TNZ-hemihydrate, the water molecule was found to be disordered and refined with two alternative positions (0.5 site-occupancy factor for both components). The H atoms on the O atoms were constrained using the command AFIX6, with their U_{iso} fixed at 1.5U_{eq}(O).

7. Theoretical calculations

A conformational search for the neutral molecules of tinidazole was performed using *Mercury* (Macrae *et al.*, 2020), considering all rotatable bonds. The 200 conformations suggested by the program were subsequently subjected to DFT calculations using *GAUSSIAN09* (Frisch *et al.*, 2013) at the B3LYP-GD3BJ/6-311G(d,p) level of theory (Becke, 1993;

Grimme *et al.*, 2011; Johnson & Becke, 2006). The optimized geometries were confirmed as stationary points by the absence of imaginary vibrational frequencies. In some cases, a single low-magnitude imaginary frequency (<11*i* cm^{-1}) was observed (Table S1 in the supporting information). Final Cartesian coordinates (X, Y, Z in Å) for the optimized TNZ conformers are listed in Tables S6–S59 in the supporting information.

Single-point energy calculations were also performed using the same level of theory for five independent tinidazole molecules extracted from the crystal structures of TNZ-monoclinic, TNZ-triclinic and TNZ-hemihydrate forms, to put the results of conformational analysis into perspective. Prior to DFT calculations, hydrogen-atom positions were normalized according to the values reported by Allen & Bruno (2010). Cartesian coordinates (X, Y, Z in Å) for the TNZ-molecules taken from the crystal structures of TNZ-monoclinic, TNZ-triclinic and TNZ-hemihydrate are listed in Tables S60–S64 in the supporting information.

Acknowledgements

The financial support from University of Lodz Doctoral School of Exact and Natural Sciences is gratefully acknowledged.

References

Alfaro-Fuentes, I., López-Sandoval, H., Mijangos, E., Duarte-Hernández, A. M., Rodriguez-López, G., Bernal-Uruchurtu, M. I., Contreras, R., Flores-Parra, A. & Barba-Behrens, N. (2014). *Polyhedron* **67**, 373–380.

Allen, F. H. & Bruno, I. J. (2010). *Acta Cryst.* B**66**, 380–386.

Ang, C. W., Jarrad, A. M., Cooper, M. A. & Blaskovich, A. T. (2017). *J. Med. Chem.* **60**, 7636–7657.

Becke, A. D. (1993). *J. Chem. Phys.* **98**, 5648–5652.

Ben, A. & Chęcińska, L. (2025). *Acta Cryst.* E**81**, 1018–1022.

Bernstein, J., Davis, R. E., Shimoni, L. & Chang, N. L. (1995). *Angew. Chem. Int. Ed. Engl.* **34**, 1555–1573.

Chasseaud, L. F., Henrick, K., Matthews, R. W., Scott, P. W. & Wood, S. G. (1984). *J. Chem. Soc. Chem. Commun.* pp. 491–492.

Crowell, A. L., Sanders-Lewis, K. A. & Secor, W. E. (2003). *Antimicrob. Agents Chemother.* **47**, 1407–1409.

Etter, M. C. (1990). *Acc. Chem. Res.* **23**, 120–126.

Etter, M. C., MacDonald, J. C. & Bernstein, J. (1990). *Acta Cryst.* B**46**, 256–262.

Fandiño, O. E., Reviglio, L., Linck, Y. G., Monti, G. A., Marcos Valdez, M. M., Faudone, S. N., Caira, M. R. & Sperandeo, N. R. (2020). *Cryst. Growth Des.* **20**, 2930–2942.

Frisch, M. J., Trucks, G. W., Schlegel, H. B., Scuseria, G. E., Robb, M. A., Cheeseman, J. R., Scalmani, G., Barone, V., Mennucci, B., Petersson, G. A., Nakatsuji, H., Caricato, M., Li, X., Hratchian, H. P., Izmaylov, A. F., Bloino, J., Zheng, G., Sonnenberg, J. L., Hada, M., Ehara, M., Toyota, K., Fukuda, R., Hasegawa, J., Ishida, M., Nakajima, T., Honda, Y., Kitao, O., Nakai, H., Vreven, T., Montgomery, J. A. Jr, Peralta, J. E., Ogliaro, F., Bearpark, M., Heyd, J. J., Brothers, E., Kudin, K. N., Staroverov, V. N., Keith, T., Kobayashi, R., Normand, J., Raghavachari, K., Rendell, A., Burant, J. C., Iyengar, S. S., Tomasi, J., Cossi, M., Rega, N., Millam, J. M., Klene, M., Knox, J. E., Cross, J. B., Bakken, V., Adamo, C., Jaramillo, J., Gomperts, R., Stratmann, R. E., Yazyev, O., Austin, A. J., Cammi, R., Pomelli, C., Ochterski, J. W., Martin, R. L., Morokuma, K., Zakrzewski, V. G., Voth, G. A., Salvador, P., Dannenberg, J. J., Dapprich, S., Daniels, A. D., Farkas, O., Foresman, J. B., Ortiz, J. V., Cioslowski, J. & Fox, D. J. (2013). *GAUSSIAN09*. Revision D. 01. Gaussian Inc., Wallingford CT, USA. https://gaussian.com/.

Fung, H. B. & Doan, T. L. (2005). *Clin. Ther.* **27**, 1859–1884.

Gardner, T. B. & Hill, D. R. (2001). *Clin. Microbiol. Rev.* **14**, 114–128.

Grimme, S., Ehrlich, S. & Goerigk, L. (2011). *J. Comput. Chem.* **32**, 1456–1465.

Groom, C. R., Bruno, I. J., Lightfoot, M. P. & Ward, S. C. (2016). *Acta Cryst.* B**72**, 171–179.

Johnson, E. R. & Becke, A. D. (2006). *J. Chem. Phys.* **124**, 174104.

Li, N., Chen, R., Zhang, M., Wu, T. & Liu, K. (2023). *CSD Communication* (refcode NIJCOC). CCDC, Cambridge, England.

Mackenzie, C. F., Spackman, P. R., Jayatilaka, D. & Spackman, M. A. (2017). *IUCrJ* **4**, 575–587.

Macrae, C. F., Sovago, I., Cottrell, S. J., Galek, P. T. A., McCabe, P., Pidcock, E., Platings, M., Shields, G. P., Stevens, J. S., Towler, M. & Wood, P. A. (2020). *J. Appl. Cryst.* **53**, 226–235.

Nakamura, S. (1955). *Pharm. Bull.* **3**, 379–383.

Rigaku OD (2023). *CrysAlis PRO*. Rigaku Oxford Diffraction, Yarnton, England.

Rigaku OD (2025). *CrysAlis PRO*. Rigaku Oxford Diffraction, Yarnton, England.

Sawyer, P. R., Brogden, R. N., Pinder, R. M., Speight, T. M. & Avery, G. S. (1976). *Drugs* **11**, 423–440.

Sheldrick, G. M. (2015*a*). *Acta Cryst.* A**71**, 3–8.

Sheldrick, G. M. (2015*b*). *Acta Cryst.* C**71**, 3–8.

Spackman, M. A. & Jayatilaka, D. (2009). *CrystEngComm* **11**, 19–32.

Spackman, M. A. & McKinnon, J. J. (2002). *CrystEngComm* **4**, 378–392.

Spackman, P. R., Turner, M. J., McKinnon, J. J., Wolff, S. K., Grimwood, D. J., Jayatilaka, D. & Spackman, M. A. (2021). *J. Appl. Cryst.* **54**, 1006–1011.

Spek, A. L. (2020). *Acta Cryst.* E**76**, 1–11.

Turner, M. J., Grabowsky, S., Jayatilaka, D. & Spackman, M. A. (2014). *J. Phys. Chem. Lett.* **5**, 4249–4255.

Turner, M. J., Thomas, S. P., Shi, M. W., Jayatilaka, D. & Spackman, M. A. (2015). *Chem. Commun.* **51**, 3735–3738.

Westrip, S. P. (2010). *J. Appl. Cryst.* **43**, 920–925.

Wood, B. A. & Monro, A. M. (1975). *Br. J. Vener. Dis.* **51**, 51–53. https://doi.org/10.1136/sti.51.1.51

Zheng, K., Xie, C., Li, X., Wu, W., Li, A., Qian, S. & Pang, Q. (2020). *Acta Cryst.* C**76**, 389–397.

supporting information

Acta Cryst. (2025). E**81**, 1170-1177 [https://doi.org/10.1107/S2056989025010126]

Crystal structures and conformational features of new forms of tinidazole

Valeryia Hushcha, Justyna Dominikowska and Lilianna Chęcińska

Computing details

1-[2-(Ethanesulfonyl)ethyl]-2-methyl-5-nitro-1*H*-imidazole (TNZ-monoclinic)

Crystal data

$C_8H_{13}N_3O_4S$
$M_r = 247.27$
Monoclinic, $P2_1/n$
$a = 11.9943$ (2) Å
$b = 5.5233$ (1) Å
$c = 16.8454$ (2) Å
$\beta = 97.499$ (1)°
$V = 1106.43$ (3) Å^3
$Z = 4$
$F(000) = 520$
$D_x = 1.484$ Mg m^{-3}
Cu $K\alpha$ radiation, $\lambda = 1.54184$ Å
Cell parameters from 8802 reflections
$\theta = 3.7$–$76.7°$
$\mu = 2.69$ mm^{-1}
$T = 294$ K
Prism, colourless
0.27 × 0.06 × 0.04 mm

Data collection

Rigaku XtaLAB Synergy, Dualflex, HyPix diffractometer
Radiation source: micro-focus sealed X-ray tube, PhotonJet (Cu) X-ray Source
Mirror monochromator
Detector resolution: 10.0000 pixels mm^{-1}
ω scans
Absorption correction: gaussian (CrysAlisPro 1.171.42.88a; Rigaku OD, 2023)
$T_{min} = 0.208$, $T_{max} = 1.000$
10724 measured reflections
2118 independent reflections
2011 reflections with $I > 2\sigma(I)$
$R_{int} = 0.022$
$\theta_{max} = 72.1°$, $\theta_{min} = 4.3°$
$h = -14 \rightarrow 14$
$k = -6 \rightarrow 5$
$l = -20 \rightarrow 20$

Refinement

Refinement on F^2
Least-squares matrix: full
$R[F^2 > 2\sigma(F^2)] = 0.028$
$wR(F^2) = 0.081$
$S = 1.08$
2118 reflections
148 parameters
0 restraints
Primary atom site location: structure-invariant direct methods
Hydrogen site location: inferred from neighbouring sites
H-atom parameters constrained
$w = 1/[\sigma^2(F_o^2) + (0.0448P)^2 + 0.258P]$ where $P = (F_o^2 + 2F_c^2)/3$
$(\Delta/\sigma)_{max} < 0.001$
$\Delta\rho_{max} = 0.22$ e Å^{-3}
$\Delta\rho_{min} = -0.22$ e Å^{-3}
Extinction correction: SHELXL-2019/2 (Sheldrick 2015b), $Fc^* = kFc[1+0.001xFc^2\lambda^3/\sin(2\theta)]^{-1/4}$
Extinction coefficient: 0.0032 (4)

Special details

Geometry. All esds (except the esd in the dihedral angle between two l.s. planes) are estimated using the full covariance matrix. The cell esds are taken into account individually in the estimation of esds in distances, angles and torsion angles; correlations between esds in cell parameters are only used when they are defined by crystal symmetry. An approximate (isotropic) treatment of cell esds is used for estimating esds involving l.s. planes.

Fractional atomic coordinates and isotropic or equivalent isotropic displacement parameters (Å²)

	x	*y*	*z*	U_{iso}*/U_{eq}
S1	0.03059 (3)	0.16011 (6)	0.39070 (2)	0.03666 (14)
O1	0.42652 (13)	0.8226 (2)	0.43028 (8)	0.0750 (4)
O2	0.32312 (11)	0.5198 (3)	0.38502 (7)	0.0742 (4)
O3	0.04594 (10)	−0.09214 (19)	0.41130 (6)	0.0530 (3)
O4	−0.08151 (8)	0.2575 (2)	0.38353 (6)	0.0528 (3)
N1	0.38083 (10)	0.5737 (2)	0.65305 (7)	0.0446 (3)
N2	0.29935 (9)	0.3847 (2)	0.54357 (6)	0.0339 (2)
N3	0.36965 (11)	0.6432 (3)	0.44040 (8)	0.0490 (3)
C1	0.40961 (12)	0.6894 (3)	0.58822 (9)	0.0456 (3)
H1	0.456123	0.824475	0.589665	0.055*
C2	0.36016 (11)	0.5784 (3)	0.52011 (8)	0.0391 (3)
C3	0.31386 (11)	0.3923 (3)	0.62476 (8)	0.0365 (3)
C4	0.25958 (14)	0.2226 (3)	0.67572 (9)	0.0480 (4)
H4A	0.179988	0.251558	0.669057	0.072*
H4B	0.289754	0.246947	0.730774	0.072*
H4C	0.273755	0.059203	0.660413	0.072*
C5	0.22722 (11)	0.2145 (2)	0.49345 (8)	0.0358 (3)
H5A	0.215666	0.069870	0.523997	0.043*
H5B	0.263587	0.167511	0.447640	0.043*
C6	0.11443 (10)	0.3321 (2)	0.46491 (7)	0.0321 (3)
H6A	0.127442	0.491009	0.443368	0.039*
H6B	0.073507	0.354111	0.510396	0.039*
C7	0.08610 (14)	0.2091 (3)	0.29962 (8)	0.0477 (4)
H7A	0.165436	0.168332	0.307386	0.057*
H7B	0.048995	0.100205	0.259364	0.057*
C8	0.07285 (17)	0.4664 (3)	0.26841 (9)	0.0610 (5)
H8A	0.116133	0.573974	0.305129	0.092*
H8B	−0.005002	0.511921	0.263308	0.092*
H8C	0.099019	0.476101	0.217024	0.092*

Atomic displacement parameters (Å²)

	U^{11}	U^{22}	U^{33}	U^{12}	U^{13}	U^{23}
S1	0.0409 (2)	0.0338 (2)	0.0333 (2)	−0.00394 (12)	−0.00236 (13)	−0.00431 (11)
O1	0.0962 (10)	0.0667 (9)	0.0654 (8)	−0.0238 (7)	0.0232 (7)	0.0158 (6)
O2	0.0706 (8)	0.1125 (12)	0.0389 (6)	−0.0288 (8)	0.0045 (5)	0.0036 (7)
O3	0.0749 (8)	0.0319 (5)	0.0503 (6)	−0.0078 (5)	0.0012 (5)	−0.0031 (5)
O4	0.0366 (5)	0.0654 (7)	0.0532 (6)	−0.0017 (5)	−0.0059 (4)	−0.0076 (5)
N1	0.0453 (7)	0.0467 (7)	0.0402 (6)	−0.0066 (5)	−0.0003 (5)	−0.0040 (5)

N2	0.0311 (5)	0.0358 (6)	0.0334 (5)	−0.0001 (4)	−0.0006 (4)	−0.0002 (4)
N3	0.0445 (7)	0.0586 (8)	0.0441 (7)	−0.0006 (6)	0.0075 (5)	0.0086 (6)
C1	0.0435 (8)	0.0428 (8)	0.0496 (8)	−0.0086 (6)	0.0031 (6)	−0.0016 (6)
C2	0.0375 (7)	0.0402 (7)	0.0394 (7)	−0.0011 (6)	0.0045 (5)	0.0040 (6)
C3	0.0349 (6)	0.0390 (7)	0.0344 (6)	0.0013 (5)	−0.0003 (5)	−0.0011 (5)
C4	0.0563 (9)	0.0489 (8)	0.0386 (7)	−0.0067 (7)	0.0048 (6)	0.0021 (7)
C5	0.0376 (7)	0.0323 (6)	0.0360 (6)	0.0025 (5)	−0.0008 (5)	−0.0053 (5)
C6	0.0345 (6)	0.0300 (6)	0.0308 (6)	0.0010 (5)	0.0002 (5)	−0.0040 (5)
C7	0.0612 (9)	0.0495 (8)	0.0314 (7)	0.0021 (7)	0.0019 (6)	−0.0068 (6)
C8	0.0859 (13)	0.0590 (11)	0.0367 (8)	−0.0007 (9)	0.0025 (7)	0.0073 (7)

Geometric parameters (Å, º)

S1—O4	1.4385 (11)	C4—H4A	0.9600
S1—O3	1.4418 (11)	C4—H4B	0.9600
S1—C7	1.7711 (15)	C4—H4C	0.9600
S1—C6	1.7746 (12)	C5—C6	1.5210 (17)
O1—N3	1.2273 (18)	C5—H5A	0.9700
O2—N3	1.2288 (19)	C5—H5B	0.9700
N1—C3	1.3330 (18)	C6—H6A	0.9700
N1—C1	1.348 (2)	C6—H6B	0.9700
N2—C3	1.3566 (17)	C7—C8	1.516 (2)
N2—C2	1.3813 (18)	C7—H7A	0.9700
N2—C5	1.4678 (16)	C7—H7B	0.9700
N3—C2	1.4086 (18)	C8—H8A	0.9600
C1—C2	1.366 (2)	C8—H8B	0.9600
C1—H1	0.9300	C8—H8C	0.9600
C3—C4	1.478 (2)		
O4—S1—O3	118.05 (7)	H4A—C4—H4C	109.5
O4—S1—C7	108.85 (7)	H4B—C4—H4C	109.5
O3—S1—C7	107.79 (7)	N2—C5—C6	109.96 (10)
O4—S1—C6	107.24 (6)	N2—C5—H5A	109.7
O3—S1—C6	107.76 (6)	C6—C5—H5A	109.7
C7—S1—C6	106.62 (7)	N2—C5—H5B	109.7
C3—N1—C1	105.83 (12)	C6—C5—H5B	109.7
C3—N2—C2	105.16 (11)	H5A—C5—H5B	108.2
C3—N2—C5	126.02 (11)	C5—C6—S1	113.13 (9)
C2—N2—C5	128.69 (11)	C5—C6—H6A	109.0
O1—N3—O2	123.21 (14)	S1—C6—H6A	109.0
O1—N3—C2	116.94 (14)	C5—C6—H6B	109.0
O2—N3—C2	119.84 (13)	S1—C6—H6B	109.0
N1—C1—C2	109.79 (13)	H6A—C6—H6B	107.8
N1—C1—H1	125.1	C8—C7—S1	114.16 (11)
C2—C1—H1	125.1	C8—C7—H7A	108.7
C1—C2—N2	107.15 (12)	S1—C7—H7A	108.7
C1—C2—N3	127.33 (14)	C8—C7—H7B	108.7
N2—C2—N3	125.51 (13)	S1—C7—H7B	108.7

N1—C3—N2	112.06 (12)	H7A—C7—H7B	107.6
N1—C3—C4	124.03 (12)	C7—C8—H8A	109.5
N2—C3—C4	123.90 (12)	C7—C8—H8B	109.5
C3—C4—H4A	109.5	H8A—C8—H8B	109.5
C3—C4—H4B	109.5	C7—C8—H8C	109.5
H4A—C4—H4B	109.5	H8A—C8—H8C	109.5
C3—C4—H4C	109.5	H8B—C8—H8C	109.5
C3—N1—C1—C2	−0.03 (17)	C2—N2—C3—N1	−1.16 (15)
N1—C1—C2—N2	−0.68 (17)	C5—N2—C3—N1	−177.30 (11)
N1—C1—C2—N3	−179.68 (13)	C2—N2—C3—C4	177.50 (13)
C3—N2—C2—C1	1.08 (15)	C5—N2—C3—C4	1.4 (2)
C5—N2—C2—C1	177.08 (12)	C3—N2—C5—C6	97.29 (15)
C3—N2—C2—N3	−179.89 (13)	C2—N2—C5—C6	−77.93 (16)
C5—N2—C2—N3	−3.9 (2)	N2—C5—C6—S1	170.06 (8)
O1—N3—C2—C1	−1.8 (2)	O4—S1—C6—C5	166.17 (10)
O2—N3—C2—C1	177.36 (16)	O3—S1—C6—C5	38.12 (12)
O1—N3—C2—N2	179.39 (14)	C7—S1—C6—C5	−77.36 (11)
O2—N3—C2—N2	−1.5 (2)	O4—S1—C7—C8	49.01 (14)
C1—N1—C3—N2	0.76 (16)	O3—S1—C7—C8	178.16 (12)
C1—N1—C3—C4	−177.90 (14)	C6—S1—C7—C8	−66.38 (13)

Hydrogen-bond geometry (Å, º)

D—H···*A*	*D*—H	H···*A*	*D*···*A*	*D*—H···*A*
C1—H1···O1^{i}	0.93	2.45	3.374 (2)	171
C6—H6*A*···O3^{ii}	0.97	2.53	3.3777 (17)	146
C6—H6*B*···O3^{iii}	0.97	2.53	3.2942 (17)	136

Symmetry codes: (i) −*x*+1, −*y*+2, −*z*+1; (ii) *x*, *y*+1, *z*; (iii) −*x*, −*y*, −*z*+1.

1-[2-(Ethanesulfonyl)ethyl]-2-methyl-5-nitro-1*H*-imidazole (TNZ-triclinic)

Crystal data

$C_8H_{13}N_3O_4S$
M_r = 247.27
Triclinic, $P\overline{1}$
a = 5.7208 (2) Å
b = 13.2759 (5) Å
c = 15.5932 (5) Å
α = 77.101 (3)°
β = 85.407 (2)°
γ = 77.923 (3)°
V = 1128.16 (7) Å^3
Z = 4
$F(000)$ = 520
D_x = 1.456 Mg m^{-3}
Cu $K\alpha$ radiation, λ = 1.54184 Å
Cell parameters from 6574 reflections
θ = 2.9–76.0°
μ = 2.64 mm^{-1}
T = 294 K
Needle, colourless
0.23 × 0.04 × 0.02 mm

Data collection

Rigaku XtaLAB Synergy, Dualflex, HyPix diffractometer
Radiation source: micro-focus sealed X-ray tube, PhotonJet (Cu) X-ray Source
Mirror monochromator
Detector resolution: 10.0000 pixels mm^{-1}
ω scans
Absorption correction: gaussian (CrysAlisPro 1.171.42.88a; Rigaku OD, 2023)
T_{min} = 0.496, T_{max} = 1.000

11280 measured reflections
4260 independent reflections
3758 reflections with $I > 2\sigma(I)$
$R_{int} = 0.032$
$\theta_{max} = 72.1°$, $\theta_{min} = 2.9°$
$h = -5 \rightarrow 6$
$k = -16 \rightarrow 16$
$l = -19 \rightarrow 19$

Refinement

Refinement on F^2
Least-squares matrix: full
$R[F^2 > 2\sigma(F^2)] = 0.039$
$wR(F^2) = 0.103$
$S = 1.03$
4260 reflections
293 parameters
0 restraints
Primary atom site location: structure-invariant direct methods
Hydrogen site location: inferred from neighbouring sites
H-atom parameters constrained
$w = 1/[\sigma^2(F_o^2) + (0.0533P)^2 + 0.3451P]$ where $P = (F_o^2 + 2F_c^2)/3$
$(\Delta/\sigma)_{max} < 0.001$
$\Delta\rho_{max} = 0.20$ e Å^{-3}
$\Delta\rho_{min} = -0.34$ e Å^{-3}

Special details

Geometry. All esds (except the esd in the dihedral angle between two l.s. planes) are estimated using the full covariance matrix. The cell esds are taken into account individually in the estimation of esds in distances, angles and torsion angles; correlations between esds in cell parameters are only used when they are defined by crystal symmetry. An approximate (isotropic) treatment of cell esds is used for estimating esds involving l.s. planes.

Fractional atomic coordinates and isotropic or equivalent isotropic displacement parameters (Å²)

	x	*y*	*z*	U_{iso}*/U_{eq}
S1	0.08813 (8)	0.71568 (4)	0.16126 (3)	0.03887 (13)
O1	0.6015 (3)	0.35548 (15)	0.08904 (12)	0.0659 (5)
O2	0.2507 (3)	0.43620 (14)	0.04360 (11)	0.0615 (4)
O3	0.3279 (3)	0.66741 (13)	0.18638 (12)	0.0643 (5)
O4	−0.0825 (3)	0.73682 (14)	0.23036 (11)	0.0658 (5)
N1	0.3266 (3)	0.39747 (15)	0.33339 (12)	0.0525 (4)
N2	0.1110 (3)	0.46958 (12)	0.21403 (10)	0.0372 (3)
N3	0.3968 (3)	0.40279 (13)	0.10195 (12)	0.0446 (4)
C1	0.4581 (4)	0.37273 (17)	0.26206 (15)	0.0480 (5)
H1	0.612177	0.332307	0.263463	0.058*
C2	0.3309 (3)	0.41597 (14)	0.18791 (13)	0.0390 (4)
C3	0.1200 (4)	0.45513 (16)	0.30271 (14)	0.0445 (4)
C4	−0.0803 (5)	0.4971 (2)	0.35979 (17)	0.0616 (6)
H4A	−0.035545	0.475548	0.420169	0.092*
H4B	−0.219289	0.470259	0.352702	0.092*
H4C	−0.115617	0.572689	0.343391	0.092*
C5	−0.0842 (3)	0.53641 (15)	0.15968 (14)	0.0413 (4)
H5A	−0.219792	0.556701	0.197978	0.050*
H5B	−0.133638	0.495553	0.122507	0.050*
C6	−0.0180 (4)	0.63580 (15)	0.10156 (13)	0.0421 (4)
H6A	−0.157448	0.677088	0.069842	0.050*
H6B	0.104571	0.615625	0.058473	0.050*
C7	0.0924 (4)	0.83392 (17)	0.08253 (15)	0.0518 (5)
H7A	0.179742	0.817786	0.029758	0.062*
H7B	−0.070161	0.868092	0.066767	0.062*

C8	0.2082 (5)	0.90791 (19)	0.11768 (17)	0.0636 (6)
H8A	0.126938	0.921067	0.171570	0.095*
H8B	0.198259	0.973191	0.075238	0.095*
H8C	0.373046	0.876575	0.128607	0.095*
S2	0.37980 (7)	−0.12502 (4)	0.38486 (3)	0.03747 (13)
O5	0.3989 (3)	0.15492 (15)	0.04148 (11)	0.0672 (5)
O6	0.6738 (3)	0.07162 (15)	0.13344 (11)	0.0662 (5)
O7	0.1508 (2)	−0.08429 (13)	0.34643 (11)	0.0555 (4)
O8	0.3992 (3)	−0.11542 (14)	0.47345 (10)	0.0598 (4)
N4	−0.0068 (3)	0.21724 (14)	0.25810 (13)	0.0500 (4)
N5	0.3589 (2)	0.11938 (12)	0.27507 (10)	0.0359 (3)
N6	0.4724 (3)	0.12279 (14)	0.11701 (11)	0.0463 (4)
C11	0.0886 (4)	0.20747 (17)	0.17801 (15)	0.0479 (5)
H11	0.012668	0.237178	0.125129	0.057*
C12	0.3125 (3)	0.14772 (15)	0.18598 (12)	0.0384 (4)
C13	0.1580 (3)	0.16381 (15)	0.31583 (14)	0.0419 (4)
C14	0.1216 (4)	0.1555 (2)	0.41149 (15)	0.0580 (6)
H14A	−0.041359	0.185720	0.424524	0.087*
H14B	0.226514	0.192617	0.431389	0.087*
H14C	0.156027	0.082606	0.440929	0.087*
C15	0.5715 (3)	0.05185 (16)	0.31960 (13)	0.0408 (4)
H15A	0.562506	0.058683	0.380487	0.049*
H15B	0.712940	0.076557	0.291887	0.049*
C16	0.5981 (3)	−0.06392 (16)	0.31728 (14)	0.0409 (4)
H16A	0.756089	−0.101049	0.336541	0.049*
H16B	0.585441	−0.070028	0.257059	0.049*
C17	0.4715 (4)	−0.25926 (17)	0.37811 (16)	0.0545 (5)
H17A	0.467919	−0.265187	0.317362	0.065*
H17B	0.634963	−0.284489	0.396862	0.065*
C18	0.3141 (6)	−0.3267 (2)	0.4341 (2)	0.0834 (9)
H18A	0.327090	−0.325432	0.494834	0.125*
H18B	0.362940	−0.397781	0.426043	0.125*
H18C	0.151149	−0.300131	0.417356	0.125*

Atomic displacement parameters (Å²)

	U^{11}	U^{22}	U^{33}	U^{12}	U^{13}	U^{23}
S1	0.0419 (3)	0.0380 (2)	0.0388 (2)	−0.01155 (19)	−0.00137 (18)	−0.00918 (18)
O1	0.0476 (9)	0.0757 (11)	0.0699 (11)	0.0028 (8)	0.0091 (8)	−0.0241 (9)
O2	0.0660 (10)	0.0653 (10)	0.0539 (9)	0.0017 (8)	−0.0151 (8)	−0.0235 (8)
O3	0.0525 (9)	0.0580 (10)	0.0845 (12)	−0.0083 (7)	−0.0290 (8)	−0.0122 (8)
O4	0.0839 (12)	0.0631 (10)	0.0604 (10)	−0.0320 (9)	0.0282 (8)	−0.0282 (8)
N1	0.0580 (11)	0.0486 (10)	0.0486 (10)	−0.0066 (8)	−0.0104 (8)	−0.0063 (8)
N2	0.0351 (8)	0.0330 (8)	0.0444 (9)	−0.0081 (6)	−0.0017 (6)	−0.0083 (6)
N3	0.0442 (9)	0.0394 (9)	0.0519 (10)	−0.0074 (7)	−0.0008 (7)	−0.0142 (7)
C1	0.0435 (11)	0.0446 (11)	0.0550 (12)	−0.0042 (9)	−0.0088 (9)	−0.0100 (9)
C2	0.0361 (9)	0.0351 (9)	0.0473 (10)	−0.0080 (7)	−0.0014 (8)	−0.0106 (8)
C3	0.0510 (11)	0.0369 (10)	0.0464 (11)	−0.0127 (8)	0.0007 (9)	−0.0074 (8)

C4	0.0674 (15)	0.0615 (14)	0.0545 (13)	−0.0129 (12)	0.0131 (11)	−0.0146 (11)
C5	0.0318 (9)	0.0400 (10)	0.0542 (11)	−0.0068 (7)	−0.0064 (8)	−0.0126 (9)
C6	0.0425 (10)	0.0398 (10)	0.0448 (10)	−0.0049 (8)	−0.0096 (8)	−0.0109 (8)
C7	0.0632 (13)	0.0452 (11)	0.0484 (12)	−0.0201 (10)	−0.0047 (10)	−0.0031 (9)
C8	0.0848 (17)	0.0508 (13)	0.0629 (15)	−0.0309 (12)	0.0024 (12)	−0.0132 (11)
S2	0.0268 (2)	0.0443 (3)	0.0422 (3)	−0.00891 (17)	0.00138 (17)	−0.01027 (19)
O5	0.0749 (11)	0.0832 (12)	0.0417 (9)	−0.0178 (9)	−0.0001 (8)	−0.0083 (8)
O6	0.0485 (9)	0.0793 (12)	0.0586 (10)	0.0029 (8)	0.0110 (7)	−0.0081 (8)
O7	0.0262 (7)	0.0632 (10)	0.0777 (11)	−0.0106 (6)	−0.0057 (6)	−0.0129 (8)
O8	0.0719 (10)	0.0717 (10)	0.0418 (8)	−0.0265 (8)	0.0025 (7)	−0.0150 (7)
N4	0.0349 (8)	0.0463 (10)	0.0644 (11)	−0.0033 (7)	0.0005 (8)	−0.0080 (8)
N5	0.0291 (7)	0.0379 (8)	0.0409 (8)	−0.0077 (6)	0.0009 (6)	−0.0085 (6)
N6	0.0471 (10)	0.0475 (10)	0.0447 (9)	−0.0150 (8)	0.0048 (7)	−0.0076 (7)
C11	0.0393 (10)	0.0488 (12)	0.0524 (12)	−0.0083 (9)	−0.0065 (9)	−0.0026 (9)
C12	0.0347 (9)	0.0397 (10)	0.0413 (10)	−0.0114 (7)	0.0013 (7)	−0.0070 (8)
C13	0.0348 (9)	0.0392 (10)	0.0519 (11)	−0.0090 (8)	0.0045 (8)	−0.0105 (8)
C14	0.0567 (13)	0.0627 (14)	0.0538 (13)	−0.0071 (11)	0.0126 (10)	−0.0197 (11)
C15	0.0273 (8)	0.0488 (11)	0.0475 (11)	−0.0113 (8)	−0.0046 (7)	−0.0082 (8)
C16	0.0224 (8)	0.0465 (11)	0.0500 (11)	−0.0050 (7)	0.0027 (7)	−0.0057 (8)
C17	0.0534 (12)	0.0468 (12)	0.0616 (14)	−0.0098 (10)	0.0108 (10)	−0.0124 (10)
C18	0.098 (2)	0.0563 (15)	0.098 (2)	−0.0314 (15)	0.0356 (17)	−0.0194 (15)

Geometric parameters (Å, º)

S1—O4	1.4298 (17)	S2—O8	1.4304 (16)
S1—O3	1.4322 (16)	S2—O7	1.4324 (14)
S1—C7	1.767 (2)	S2—C17	1.774 (2)
S1—C6	1.7777 (19)	S2—C16	1.7777 (18)
O1—N3	1.232 (2)	O5—N6	1.235 (2)
O2—N3	1.229 (2)	O6—N6	1.224 (2)
N1—C3	1.327 (3)	N4—C13	1.332 (3)
N1—C1	1.356 (3)	N4—C11	1.345 (3)
N2—C3	1.357 (3)	N5—C13	1.356 (2)
N2—C2	1.388 (2)	N5—C12	1.388 (2)
N2—C5	1.468 (2)	N5—C15	1.472 (2)
N3—C2	1.402 (3)	N6—C12	1.406 (3)
C1—C2	1.364 (3)	C11—C12	1.357 (3)
C1—H1	0.9300	C11—H11	0.9300
C3—C4	1.486 (3)	C13—C14	1.472 (3)
C4—H4A	0.9600	C14—H14A	0.9600
C4—H4B	0.9600	C14—H14B	0.9600
C4—H4C	0.9600	C14—H14C	0.9600
C5—C6	1.525 (3)	C15—C16	1.521 (3)
C5—H5A	0.9700	C15—H15A	0.9700
C5—H5B	0.9700	C15—H15B	0.9700
C6—H6A	0.9700	C16—H16A	0.9700
C6—H6B	0.9700	C16—H16B	0.9700
C7—C8	1.508 (3)	C17—C18	1.496 (3)

C7—H7A	0.9700	C17—H17A	0.9700
C7—H7B	0.9700	C17—H17B	0.9700
C8—H8A	0.9600	C18—H18A	0.9600
C8—H8B	0.9600	C18—H18B	0.9600
C8—H8C	0.9600	C18—H18C	0.9600
O4—S1—O3	116.91 (12)	O8—S2—O7	116.91 (10)
O4—S1—C7	109.09 (11)	O8—S2—C17	109.27 (11)
O3—S1—C7	109.09 (11)	O7—S2—C17	109.04 (11)
O4—S1—C6	108.83 (10)	O8—S2—C16	108.63 (10)
O3—S1—C6	108.82 (10)	O7—S2—C16	109.06 (9)
C7—S1—C6	103.23 (10)	C17—S2—C16	103.02 (10)
C3—N1—C1	105.66 (17)	C13—N4—C11	106.46 (17)
C3—N2—C2	104.93 (16)	C13—N5—C12	105.21 (15)
C3—N2—C5	125.70 (16)	C13—N5—C15	125.44 (16)
C2—N2—C5	129.15 (16)	C12—N5—C15	129.29 (15)
O2—N3—O1	122.79 (19)	O6—N6—O5	123.20 (19)
O2—N3—C2	119.86 (17)	O6—N6—C12	119.88 (17)
O1—N3—C2	117.33 (17)	O5—N6—C12	116.93 (18)
N1—C1—C2	109.84 (18)	N4—C11—C12	109.74 (18)
N1—C1—H1	125.1	N4—C11—H11	125.1
C2—C1—H1	125.1	C12—C11—H11	125.1
C1—C2—N2	107.05 (18)	C11—C12—N5	107.15 (17)
C1—C2—N3	127.48 (18)	C11—C12—N6	126.68 (18)
N2—C2—N3	125.28 (17)	N5—C12—N6	126.12 (16)
N1—C3—N2	112.52 (18)	N4—C13—N5	111.44 (18)
N1—C3—C4	123.4 (2)	N4—C13—C14	123.19 (18)
N2—C3—C4	124.04 (19)	N5—C13—C14	125.37 (18)
C3—C4—H4A	109.5	C13—C14—H14A	109.5
C3—C4—H4B	109.5	C13—C14—H14B	109.5
H4A—C4—H4B	109.5	H14A—C14—H14B	109.5
C3—C4—H4C	109.5	C13—C14—H14C	109.5
H4A—C4—H4C	109.5	H14A—C14—H14C	109.5
H4B—C4—H4C	109.5	H14B—C14—H14C	109.5
N2—C5—C6	113.80 (14)	N5—C15—C16	113.50 (14)
N2—C5—H5A	108.8	N5—C15—H15A	108.9
C6—C5—H5A	108.8	C16—C15—H15A	108.9
N2—C5—H5B	108.8	N5—C15—H15B	108.9
C6—C5—H5B	108.8	C16—C15—H15B	108.9
H5A—C5—H5B	107.7	H15A—C15—H15B	107.7
C5—C6—S1	113.50 (14)	C15—C16—S2	112.98 (13)
C5—C6—H6A	108.9	C15—C16—H16A	109.0
S1—C6—H6A	108.9	S2—C16—H16A	109.0
C5—C6—H6B	108.9	C15—C16—H16B	109.0
S1—C6—H6B	108.9	S2—C16—H16B	109.0
H6A—C6—H6B	107.7	H16A—C16—H16B	107.8
C8—C7—S1	111.26 (16)	C18—C17—S2	111.82 (18)
C8—C7—H7A	109.4	C18—C17—H17A	109.3

S1—C7—H7A	109.4	S2—C17—H17A	109.3
C8—C7—H7B	109.4	C18—C17—H17B	109.3
S1—C7—H7B	109.4	S2—C17—H17B	109.3
H7A—C7—H7B	108.0	H17A—C17—H17B	107.9
C7—C8—H8A	109.5	C17—C18—H18A	109.5
C7—C8—H8B	109.5	C17—C18—H18B	109.5
H8A—C8—H8B	109.5	H18A—C18—H18B	109.5
C7—C8—H8C	109.5	C17—C18—H18C	109.5
H8A—C8—H8C	109.5	H18A—C18—H18C	109.5
H8B—C8—H8C	109.5	H18B—C18—H18C	109.5

C3—N1—C1—C2	0.2 (2)	C13—N4—C11—C12	0.2 (2)
N1—C1—C2—N2	−0.2 (2)	N4—C11—C12—N5	−0.3 (2)
N1—C1—C2—N3	−175.24 (18)	N4—C11—C12—N6	−177.69 (18)
C3—N2—C2—C1	0.0 (2)	C13—N5—C12—C11	0.3 (2)
C5—N2—C2—C1	174.68 (17)	C15—N5—C12—C11	177.49 (17)
C3—N2—C2—N3	175.23 (17)	C13—N5—C12—N6	177.69 (17)
C5—N2—C2—N3	−10.1 (3)	C15—N5—C12—N6	−5.1 (3)
O2—N3—C2—C1	170.95 (19)	O6—N6—C12—C11	176.8 (2)
O1—N3—C2—C1	−7.7 (3)	O5—N6—C12—C11	−3.1 (3)
O2—N3—C2—N2	−3.3 (3)	O6—N6—C12—N5	−0.2 (3)
O1—N3—C2—N2	178.06 (18)	O5—N6—C12—N5	179.98 (18)
C1—N1—C3—N2	−0.2 (2)	C11—N4—C13—N5	0.0 (2)
C1—N1—C3—C4	178.6 (2)	C11—N4—C13—C14	180.0 (2)
C2—N2—C3—N1	0.2 (2)	C12—N5—C13—N4	−0.2 (2)
C5—N2—C3—N1	−174.77 (16)	C15—N5—C13—N4	−177.54 (16)
C2—N2—C3—C4	−178.68 (19)	C12—N5—C13—C14	179.9 (2)
C5—N2—C3—C4	6.4 (3)	C15—N5—C13—C14	2.5 (3)
C3—N2—C5—C6	109.6 (2)	C13—N5—C15—C16	107.0 (2)
C2—N2—C5—C6	−64.0 (2)	C12—N5—C15—C16	−69.7 (2)
N2—C5—C6—S1	−56.1 (2)	N5—C15—C16—S2	−70.36 (19)
O4—S1—C6—C5	−52.97 (17)	O8—S2—C16—C15	−58.53 (16)
O3—S1—C6—C5	75.45 (17)	O7—S2—C16—C15	69.93 (16)
C7—S1—C6—C5	−168.77 (15)	C17—S2—C16—C15	−174.34 (14)
O4—S1—C7—C8	71.6 (2)	O8—S2—C17—C18	62.5 (2)
O3—S1—C7—C8	−57.2 (2)	O7—S2—C17—C18	−66.4 (2)
C6—S1—C7—C8	−172.76 (18)	C16—S2—C17—C18	177.8 (2)

Hydrogen-bond geometry (Å, º)

D—H···*A*	*D*—H	H···*A*	*D*···*A*	*D*—H···*A*
C1—H1···N4^{i}	0.93	2.39	3.319 (3)	174
C4—H4*C*···O4	0.96	2.51	3.365 (3)	148
C6—H6*B*···O2	0.97	2.41	3.057 (3)	124
C16—H16*A*···O7^{i}	0.97	2.34	3.177 (2)	145

Symmetry code: (i) *x*+1, *y*, *z*.

1-[2-(Ethanesulfonyl)ethyl]-2-methyl-5-nitro-1*H*-imidazole hemihydrate (TNZ-hemihydrate)

Crystal data

$C_8H_{13}N_3O_4S·0.5H_2O$
$M_r = 256.28$
Triclinic, $P\overline{1}$
$a = 5.7223$ (1) Å
$b = 13.1854$ (2) Å
$c = 16.2439$ (4) Å
$\alpha = 102.658$ (2)°
$\beta = 92.226$ (2)°
$\gamma = 102.484$ (2)°
$V = 1162.76$ (4) Å^3
$Z = 4$
$F(000) = 540$
$D_x = 1.464$ Mg m^{-3}
Cu $K\alpha$ radiation, $\lambda = 1.54184$ Å
Cell parameters from 6288 reflections
$\theta = 2.8$–$76.8°$
$\mu = 2.61$ mm^{-1}
$T = 294$ K
Plate, colourless
0.22 × 0.06 × 0.03 mm

Data collection

Rigaku XtaLAB Synergy, Dualflex, HyPix diffractometer
Radiation source: micro-focus sealed X-ray tube, PhotonJet (Cu) X-ray Source
Mirror monochromator
Detector resolution: 10.0000 pixels mm^{-1}
ω scans
Absorption correction: gaussian (CrysAlisPro 1.171.44.109a; Rigaku OD, 2025)
$T_{min} = 0.372$, $T_{max} = 1.000$
11604 measured reflections
4366 independent reflections
3775 reflections with $I > 2\sigma(I)$
$R_{int} = 0.029$
$\theta_{max} = 72.1°$, $\theta_{min} = 2.8°$
$h = -6 \rightarrow 6$
$k = -15 \rightarrow 16$
$l = -19 \rightarrow 19$

Refinement

Refinement on F^2
Least-squares matrix: full
$R[F^2 > 2\sigma(F^2)] = 0.037$
$wR(F^2) = 0.101$
$S = 1.06$
4366 reflections
311 parameters
0 restraints
Primary atom site location: structure-invariant direct methods
Hydrogen site location: mixed
H-atom parameters constrained
$w = 1/[\sigma^2(F_o^2) + (0.0477P)^2 + 0.3462P]$ where $P = (F_o^2 + 2F_c^2)/3$
$(\Delta/\sigma)_{max} < 0.001$
$\Delta\rho_{max} = 0.22$ e Å^{-3}
$\Delta\rho_{min} = -0.34$ e Å^{-3}

Special details

Geometry. All esds (except the esd in the dihedral angle between two l.s. planes) are estimated using the full covariance matrix. The cell esds are taken into account individually in the estimation of esds in distances, angles and torsion angles; correlations between esds in cell parameters are only used when they are defined by crystal symmetry. An approximate (isotropic) treatment of cell esds is used for estimating esds involving l.s. planes.

Fractional atomic coordinates and isotropic or equivalent isotropic displacement parameters (Å^2)

	x	*y*	*z*	U_{iso}*/U_{eq}	Occ. (<1)
S1	0.06312 (8)	0.19701 (3)	0.34587 (3)	0.03670 (13)	
O1	0.5927 (3)	0.59801 (13)	0.41560 (10)	0.0598 (4)	
O2	0.2463 (3)	0.54181 (12)	0.45934 (10)	0.0567 (4)	
O3	0.2978 (3)	0.23351 (12)	0.32065 (11)	0.0600 (4)	
O4	−0.1210 (3)	0.13782 (12)	0.28019 (10)	0.0610 (4)	
N1	0.2776 (3)	0.42349 (13)	0.18121 (11)	0.0445 (4)	
N2	0.0788 (2)	0.41595 (11)	0.29565 (9)	0.0322 (3)	
N3	0.3841 (3)	0.54354 (12)	0.40339 (11)	0.0406 (4)	

C1	0.4220 (3)	0.48625 (15)	0.24956 (13)	0.0414 (4)
H1	0.577359	0.525338	0.248263	0.050*
C2	0.3041 (3)	0.48326 (13)	0.32058 (12)	0.0345 (4)
C3	0.0728 (3)	0.38224 (14)	0.21032 (12)	0.0385 (4)
C4	−0.1373 (4)	0.31084 (18)	0.15518 (15)	0.0536 (5)
H4A	−0.097973	0.297138	0.097469	0.080*
H4B	−0.270779	0.344428	0.159738	0.080*
H4C	−0.179255	0.244658	0.172555	0.080*
C5	−0.1095 (3)	0.37753 (14)	0.34807 (13)	0.0374 (4)
H5A	−0.251378	0.336346	0.311261	0.045*
H5B	−0.152533	0.438612	0.384004	0.045*
C6	−0.0342 (3)	0.30867 (14)	0.40362 (12)	0.0389 (4)
H6A	−0.169055	0.283435	0.434042	0.047*
H6B	0.094910	0.352426	0.445184	0.047*
C7	0.0842 (4)	0.12037 (17)	0.42135 (14)	0.0505 (5)
H7A	0.180273	0.165394	0.471992	0.061*
H7B	−0.075006	0.092879	0.436917	0.061*
C8	0.1977 (5)	0.02831 (19)	0.38607 (17)	0.0630 (6)
H8A	0.105881	−0.014768	0.334811	0.094*
H8B	0.199980	−0.014396	0.426835	0.094*
H8C	0.359157	0.055656	0.374176	0.094*
S2	0.32313 (8)	0.91695 (4)	0.12417 (3)	0.03969 (14)
O5	0.3930 (3)	0.82214 (15)	0.45473 (11)	0.0687 (5)
O6	0.6570 (3)	0.85724 (15)	0.36754 (13)	0.0730 (5)
O7	0.1009 (2)	0.89156 (12)	0.16127 (11)	0.0557 (4)
O8	0.3327 (3)	0.86236 (13)	0.03818 (11)	0.0689 (5)
N4	−0.0398 (3)	0.63948 (14)	0.24541 (13)	0.0508 (4)
N5	0.3248 (3)	0.73073 (12)	0.22998 (11)	0.0392 (4)
N6	0.4578 (3)	0.81414 (14)	0.38273 (13)	0.0502 (4)
C11	0.0651 (4)	0.69415 (17)	0.32269 (15)	0.0481 (5)
H11	−0.004702	0.693030	0.373339	0.058*
C12	0.2881 (3)	0.75113 (15)	0.31547 (13)	0.0406 (4)
C13	0.1176 (3)	0.66266 (15)	0.19065 (14)	0.0433 (4)
C14	0.0703 (5)	0.6189 (2)	0.09837 (16)	0.0618 (6)
H14A	−0.079136	0.566290	0.086391	0.093*
H14B	0.198078	0.586382	0.077814	0.093*
H14C	0.061139	0.675508	0.070828	0.093*
C15	0.5312 (3)	0.77637 (17)	0.18787 (15)	0.0475 (5)
H15A	0.516369	0.735990	0.129565	0.057*
H15B	0.677263	0.768569	0.215659	0.057*
C16	0.5539 (3)	0.89331 (16)	0.18868 (15)	0.0451 (5)
H16A	0.708104	0.920972	0.169478	0.054*
H16B	0.551612	0.932516	0.246506	0.054*
C17	0.4085 (4)	1.05667 (17)	0.13349 (15)	0.0501 (5)
H17A	0.436096	1.092856	0.193017	0.060*
H17B	0.558170	1.073550	0.107963	0.060*
C18	0.2209 (5)	1.0974 (2)	0.09156 (19)	0.0675 (7)
H18A	0.197008	1.063625	0.032202	0.101*

H18B	0.273240	1.173282	0.098854	0.101*	
H18C	0.072540	1.081162	0.116810	0.101*	
O1WA	0.4788 (10)	0.4248 (4)	0.0197 (3)	0.0949 (15)	0.5
H1WA	0.519771	0.492071	0.024906	0.142*	0.5
H1WB	0.391343	0.417101	0.059977	0.142*	0.5
O1WB	0.4306 (11)	0.3534 (4)	0.0155 (3)	0.0893 (15)	0.5
H1WC	0.416298	0.380212	0.067167	0.134*	0.5
H1WD	0.486427	0.298840	0.016674	0.134*	0.5

Atomic displacement parameters (Å²)

	U^{11}	U^{22}	U^{33}	U^{12}	U^{13}	U^{23}
S1	0.0392 (2)	0.0357 (2)	0.0367 (2)	0.01152 (18)	0.00552 (18)	0.00834 (18)
O1	0.0452 (8)	0.0623 (10)	0.0577 (10)	−0.0061 (7)	−0.0044 (7)	0.0039 (8)
O2	0.0656 (10)	0.0526 (9)	0.0419 (8)	0.0033 (7)	0.0177 (7)	−0.0022 (7)
O3	0.0532 (9)	0.0593 (9)	0.0772 (11)	0.0204 (7)	0.0325 (8)	0.0246 (8)
O4	0.0734 (11)	0.0485 (8)	0.0548 (9)	0.0189 (8)	−0.0203 (8)	−0.0014 (7)
N1	0.0508 (9)	0.0448 (9)	0.0395 (9)	0.0113 (7)	0.0115 (8)	0.0114 (7)
N2	0.0322 (7)	0.0300 (7)	0.0351 (8)	0.0082 (6)	0.0058 (6)	0.0072 (6)
N3	0.0441 (9)	0.0341 (8)	0.0430 (9)	0.0095 (7)	0.0047 (7)	0.0073 (7)
C1	0.0376 (10)	0.0394 (10)	0.0473 (11)	0.0066 (8)	0.0095 (9)	0.0117 (9)
C2	0.0337 (9)	0.0310 (8)	0.0390 (10)	0.0082 (7)	0.0046 (7)	0.0076 (7)
C3	0.0443 (10)	0.0336 (9)	0.0394 (10)	0.0117 (8)	0.0034 (8)	0.0100 (8)
C4	0.0555 (13)	0.0510 (12)	0.0475 (12)	0.0057 (10)	−0.0068 (10)	0.0058 (10)
C5	0.0313 (9)	0.0357 (9)	0.0464 (11)	0.0091 (7)	0.0114 (8)	0.0093 (8)
C6	0.0418 (10)	0.0362 (9)	0.0398 (10)	0.0088 (8)	0.0138 (8)	0.0093 (8)
C7	0.0609 (13)	0.0509 (12)	0.0479 (12)	0.0220 (10)	0.0096 (10)	0.0187 (10)
C8	0.0820 (17)	0.0505 (13)	0.0653 (16)	0.0301 (12)	0.0048 (13)	0.0179 (12)
S2	0.0318 (2)	0.0425 (3)	0.0425 (3)	0.00384 (18)	0.00391 (18)	0.0095 (2)
O5	0.0777 (12)	0.0781 (12)	0.0484 (10)	0.0182 (9)	0.0013 (9)	0.0111 (9)
O6	0.0500 (10)	0.0825 (12)	0.0740 (12)	−0.0103 (8)	−0.0102 (8)	0.0200 (10)
O7	0.0271 (7)	0.0615 (9)	0.0823 (11)	0.0072 (6)	0.0107 (7)	0.0265 (8)
O8	0.0940 (13)	0.0596 (10)	0.0440 (9)	0.0077 (9)	0.0080 (9)	0.0026 (8)
N4	0.0366 (9)	0.0479 (10)	0.0684 (13)	0.0039 (7)	0.0043 (8)	0.0202 (9)
N5	0.0314 (8)	0.0354 (8)	0.0519 (10)	0.0088 (6)	0.0046 (7)	0.0110 (7)
N6	0.0462 (10)	0.0457 (9)	0.0601 (12)	0.0116 (8)	−0.0031 (9)	0.0160 (9)
C11	0.0417 (11)	0.0494 (11)	0.0570 (13)	0.0106 (9)	0.0097 (10)	0.0194 (10)
C12	0.0386 (10)	0.0367 (9)	0.0490 (11)	0.0124 (8)	0.0033 (8)	0.0119 (8)
C13	0.0364 (10)	0.0366 (10)	0.0570 (13)	0.0093 (8)	0.0004 (9)	0.0108 (9)
C14	0.0629 (14)	0.0535 (13)	0.0597 (15)	0.0039 (11)	−0.0033 (12)	0.0047 (11)
C15	0.0313 (10)	0.0517 (12)	0.0633 (14)	0.0137 (8)	0.0114 (9)	0.0163 (10)
C16	0.0265 (9)	0.0499 (11)	0.0591 (13)	0.0032 (8)	0.0056 (8)	0.0185 (10)
C17	0.0466 (11)	0.0441 (11)	0.0556 (13)	0.0024 (9)	0.0001 (10)	0.0121 (10)
C18	0.0635 (15)	0.0605 (14)	0.0835 (19)	0.0179 (12)	0.0003 (13)	0.0251 (14)
O1WA	0.097 (4)	0.125 (4)	0.072 (3)	0.039 (4)	0.032 (3)	0.025 (4)
O1WB	0.125 (4)	0.112 (4)	0.055 (2)	0.056 (4)	0.032 (3)	0.036 (3)

Geometric parameters (Å, º)

S1—O4	1.4316 (16)	S2—C17	1.772 (2)
S1—O3	1.4328 (15)	S2—C16	1.776 (2)
S1—C7	1.767 (2)	O5—N6	1.230 (3)
S1—C6	1.7742 (18)	O6—N6	1.220 (2)
O1—N3	1.237 (2)	N4—C13	1.326 (3)
O2—N3	1.227 (2)	N4—C11	1.347 (3)
N1—C3	1.332 (2)	N5—C13	1.360 (2)
N1—C1	1.353 (3)	N5—C12	1.389 (3)
N2—C3	1.356 (2)	N5—C15	1.470 (2)
N2—C2	1.386 (2)	N6—C12	1.413 (3)
N2—C5	1.472 (2)	C11—C12	1.357 (3)
N3—C2	1.406 (2)	C11—H11	0.9300
C1—C2	1.363 (3)	C13—C14	1.475 (3)
C1—H1	0.9300	C14—H14A	0.9600
C3—C4	1.480 (3)	C14—H14B	0.9600
C4—H4A	0.9600	C14—H14C	0.9600
C4—H4B	0.9600	C15—C16	1.516 (3)
C4—H4C	0.9600	C15—H15A	0.9700
C5—C6	1.524 (3)	C15—H15B	0.9700
C5—H5A	0.9700	C16—H16A	0.9700
C5—H5B	0.9700	C16—H16B	0.9700
C6—H6A	0.9700	C17—C18	1.502 (3)
C6—H6B	0.9700	C17—H17A	0.9700
C7—C8	1.513 (3)	C17—H17B	0.9700
C7—H7A	0.9700	C18—H18A	0.9600
C7—H7B	0.9700	C18—H18B	0.9600
C8—H8A	0.9600	C18—H18C	0.9600
C8—H8B	0.9600	O1WA—H1WA	0.8507
C8—H8C	0.9600	O1WA—H1WB	0.8501
S2—O8	1.4334 (17)	O1WB—H1WC	0.8506
S2—O7	1.4341 (14)	O1WB—H1WD	0.8506
O4—S1—O3	117.14 (11)	O8—S2—C17	109.38 (11)
O4—S1—C7	109.10 (11)	O7—S2—C17	109.33 (10)
O3—S1—C7	109.08 (10)	O8—S2—C16	108.76 (11)
O4—S1—C6	108.40 (9)	O7—S2—C16	108.19 (9)
O3—S1—C6	108.77 (9)	C17—S2—C16	102.94 (10)
C7—S1—C6	103.48 (9)	C13—N4—C11	106.33 (17)
C3—N1—C1	106.27 (16)	C13—N5—C12	104.78 (16)
C3—N2—C2	105.13 (15)	C13—N5—C15	125.91 (18)
C3—N2—C5	125.28 (15)	C12—N5—C15	129.19 (17)
C2—N2—C5	129.30 (15)	O6—N6—O5	123.5 (2)
O2—N3—O1	123.05 (18)	O6—N6—C12	119.7 (2)
O2—N3—C2	119.69 (16)	O5—N6—C12	116.80 (18)
O1—N3—C2	117.24 (16)	N4—C11—C12	109.71 (19)
N1—C1—C2	109.36 (17)	N4—C11—H11	125.1

N1—C1—H1	125.3	C12—C11—H11	125.1
C2—C1—H1	125.3	C11—C12—N5	107.30 (18)
C1—C2—N2	107.41 (16)	C11—C12—N6	126.5 (2)
C1—C2—N3	127.15 (17)	N5—C12—N6	126.14 (17)
N2—C2—N3	125.23 (16)	N4—C13—N5	111.88 (19)
N1—C3—N2	111.83 (17)	N4—C13—C14	123.31 (19)
N1—C3—C4	123.55 (18)	N5—C13—C14	124.81 (19)
N2—C3—C4	124.60 (18)	C13—C14—H14A	109.5
C3—C4—H4A	109.5	C13—C14—H14B	109.5
C3—C4—H4B	109.5	H14A—C14—H14B	109.5
H4A—C4—H4B	109.5	C13—C14—H14C	109.5
C3—C4—H4C	109.5	H14A—C14—H14C	109.5
H4A—C4—H4C	109.5	H14B—C14—H14C	109.5
H4B—C4—H4C	109.5	N5—C15—C16	113.65 (15)
N2—C5—C6	113.47 (14)	N5—C15—H15A	108.8
N2—C5—H5A	108.9	C16—C15—H15A	108.8
C6—C5—H5A	108.9	N5—C15—H15B	108.8
N2—C5—H5B	108.9	C16—C15—H15B	108.8
C6—C5—H5B	108.9	H15A—C15—H15B	107.7
H5A—C5—H5B	107.7	C15—C16—S2	113.79 (15)
C5—C6—S1	113.48 (13)	C15—C16—H16A	108.8
C5—C6—H6A	108.9	S2—C16—H16A	108.8
S1—C6—H6A	108.9	C15—C16—H16B	108.8
C5—C6—H6B	108.9	S2—C16—H16B	108.8
S1—C6—H6B	108.9	H16A—C16—H16B	107.7
H6A—C6—H6B	107.7	C18—C17—S2	112.26 (16)
C8—C7—S1	110.75 (16)	C18—C17—H17A	109.2
C8—C7—H7A	109.5	S2—C17—H17A	109.2
S1—C7—H7A	109.5	C18—C17—H17B	109.2
C8—C7—H7B	109.5	S2—C17—H17B	109.2
S1—C7—H7B	109.5	H17A—C17—H17B	107.9
H7A—C7—H7B	108.1	C17—C18—H18A	109.5
C7—C8—H8A	109.5	C17—C18—H18B	109.5
C7—C8—H8B	109.5	H18A—C18—H18B	109.5
H8A—C8—H8B	109.5	C17—C18—H18C	109.5
C7—C8—H8C	109.5	H18A—C18—H18C	109.5
H8A—C8—H8C	109.5	H18B—C18—H18C	109.5
H8B—C8—H8C	109.5	H1WA—O1WA—H1WB	104.4
O8—S2—O7	117.27 (11)	H1WC—O1WB—H1WD	104.6

C3—N1—C1—C2	−0.1 (2)	C13—N4—C11—C12	−0.1 (2)
N1—C1—C2—N2	0.2 (2)	N4—C11—C12—N5	−0.3 (2)
N1—C1—C2—N3	−174.74 (17)	N4—C11—C12—N6	−176.66 (17)
C3—N2—C2—C1	−0.28 (18)	C13—N5—C12—C11	0.60 (19)
C5—N2—C2—C1	173.68 (16)	C15—N5—C12—C11	176.68 (17)
C3—N2—C2—N3	174.81 (16)	C13—N5—C12—N6	176.92 (17)
C5—N2—C2—N3	−11.2 (3)	C15—N5—C12—N6	−7.0 (3)
O2—N3—C2—C1	171.23 (18)	O6—N6—C12—C11	176.4 (2)

O1—N3—C2—C1	−7.5 (3)	O5—N6—C12—C11	−3.6 (3)
O2—N3—C2—N2	−2.9 (3)	O6—N6—C12—N5	0.8 (3)
O1—N3—C2—N2	178.41 (16)	O5—N6—C12—N5	−179.24 (18)
C1—N1—C3—N2	−0.1 (2)	C11—N4—C13—N5	0.5 (2)
C1—N1—C3—C4	178.22 (18)	C11—N4—C13—C14	−179.61 (19)
C2—N2—C3—N1	0.24 (19)	C12—N5—C13—N4	−0.7 (2)
C5—N2—C3—N1	−174.04 (15)	C15—N5—C13—N4	−176.92 (17)
C2—N2—C3—C4	−178.06 (17)	C12—N5—C13—C14	179.41 (19)
C5—N2—C3—C4	7.7 (3)	C15—N5—C13—C14	3.2 (3)
C3—N2—C5—C6	109.45 (19)	C13—N5—C15—C16	105.9 (2)
C2—N2—C5—C6	−63.4 (2)	C12—N5—C15—C16	−69.4 (3)
N2—C5—C6—S1	−55.76 (19)	N5—C15—C16—S2	−68.9 (2)
O4—S1—C6—C5	−53.86 (16)	O8—S2—C16—C15	−60.75 (17)
O3—S1—C6—C5	74.51 (16)	O7—S2—C16—C15	67.64 (17)
C7—S1—C6—C5	−169.61 (14)	C17—S2—C16—C15	−176.70 (15)
O4—S1—C7—C8	72.3 (2)	O8—S2—C17—C18	71.3 (2)
O3—S1—C7—C8	−56.8 (2)	O7—S2—C17—C18	−58.4 (2)
C6—S1—C7—C8	−172.42 (17)	C16—S2—C17—C18	−173.24 (19)

Hydrogen-bond geometry (Å, º)

D—H···*A*	*D*—H	H···*A*	*D*···*A*	*D*—H···*A*
O1*WA*—H1*WB*···N1	0.85	2.09	2.908 (5)	162
O1*WB*—H1*WC*···N1	0.85	2.06	2.882 (5)	163
O1*WA*—H1*WA*···O1*WA*^{i}	0.85	1.44	2.180 (10)	143
O1*WB*—H1*WD*···O8^{i}	0.85	2.56	3.370 (5)	158
C1—H1···N4^{ii}	0.93	2.38	3.310 (3)	175
C6—H6*B*···O2	0.97	2.42	3.063 (2)	124
C14—H14*B*···O1*WA*^{i}	0.96	2.49	3.348 (6)	149
C15—H15*A*···O1*WB*^{i}	0.97	2.46	3.41 (4)	168
C16—H16*B*···O6	0.97	2.50	3.100 (3)	120
C16—H16*A*···O7^{ii}	0.97	2.37	3.183 (2)	141

Symmetry codes: (i) −*x*+1, −*y*+1, −*z*; (ii) *x*+1, *y*, *z*.